arXiv:2112.05308v2 [q-fin.PR] 14 Apr 2022

Option Pricing with State-dependent Pricing Kernel

Chen Tong[a] **Peter Reinhard Hansen**[b*] **Zhuo Huang**[c]

[a]*Department of Finance, School of Economics & Wang Yanan Institute for Studies in Economics (WISE), Xiamen University*

[b]*University of North Carolina & Copenhagen Business School*

[c]*National School of Development, Peking University*

April 15, 2022

Abstract

We introduce a new volatility model for option pricing that combines Markov switching with the Realized GARCH framework. This leads to a novel pricing kernel with a state-dependent variance risk premium and a pricing formula for European options, which is derived with an analytical approximation method. We apply the Markov switching Realized GARCH model to S&P 500 index options from 1990 to 2019 and find that investors' aversion to volatility-specific risk is time-varying. The proposed framework outperforms competing models and reduces (in-sample and out-of-sample) option pricing errors by 15% or more.

Keywords: Option Pricing, Realized GARCH, Regime-switching, Variance Risk Premium, Edgeworth Expansion

JEL Classification: G12, G13, C51, C52

*Correspondence author: Peter Reinhard Hansen (hansen@unc.edu). We would like to acknowledge the helpful comments and suggestions from Bart Frijns (the editor), Robert I. Webb, Biao Guo (discussant), and the audience at the 2021 International Conference on Derivatives and Capital Markets. We thank Emily Dyckman for proofreading the manuscript. Zhuo Huang acknowledges the financial support from the National Natural Science Foundation of China (71671004). Chen Tong's research was supported by the Fundamental Research Funds for the Central Universities (20720221025).

1 Introduction

Risk aversion is a fundamental concept in economic theory with uncertainty. It is embedded in the pricing kernel that bridges the physical probability measure, $\mathbb{P}$, with the risk-neutral measures, $\mathbb{Q}$.[1] In the classical asset pricing model with a risk-averse investor, see Lucas (1978), the pricing kernel is monotonically declining in aggregate wealth. In practice, the pricing kernel is unknown but can be estimated using a variety of econometric methods, see e.g. Aït-Sahalia and Lo (2000), Jackwerth (2000) and Rosenberg and Engle (2002). When an empirical pricing kernel is plotted against the market return, it often has a upward sloping region. This is contrary to the classical model and has become known as a *pricing kernel puzzle*. The empirical pricing kernel is typically found to be U-shaped when estimated over a long sample period, see e.g. Bakshi et al. (2010) and Christoffersen et al. (2013).

A popular explanation for the pricing kernel puzzle is the existence of additional risk factors beyond the equity risk premium. Compensation for additional risk factors can influence the projection onto the return dimension and induce the pricing kernel puzzle. A possible risk factor, which is supported by the empirical evidence, is the *variance risk premium*. The squared VIX is a measure of the squared variation under $\mathbb{Q}$ and it is, on average, larger than empirical measures of return variance under $\mathbb{P}$. When volatility is larger under the risk-neutral measure than under the physical measure it implies a negative variance risk premium, which can explain the observed U-shaped in empirical pricing kernels. An important contribution to this literature was made in Christoffersen et al. (2013), who proposed a variance-dependent pricing kernel with a variance risk premium in addition to the equity risk premium.

While pricing kernels are typically found to be U-shaped, there is also evidence that their shapes are unstable over time. In fact, there are periods when the U-shaped pricing kernel disappeared, and exhibited hump-shaped or even inverted U-shaped. Examples of this can be seen in Christoffersen et al. (2013) for their semi-parametric estimates during the year 2004 to 2007. For the same sample period, Grith et al. (2017) estimated a hump-shaped pricing kernel with DAX 30 index options. A related approach is to estimate the probability weighting function, as in Polkovnichenko and Zhao (2013). They estimate the probability weighting function to have a regular S-shaped in the same period (2004-2007) using S&P 500 index options, as opposed to an inverse S-shaped, which they estimate for most periods. The latter corresponds to a U-shaped pric-

[1] The risk-neutral measure (or equivalent martingale measure) is a probability measure such that each share price is exactly equal to the risk-free discounted expectation of the share price under this measure.

ing kernel.[2] Similarly, Kiesel and Rahe (2017) found a slight positive variance risk premium from mid-2004 to mid-2007. So, these studies suggest that the variance risk aversion was relatively low during this period.

In classical asset pricing models, the risk aversion parameter is constant over time, and this greatly simplifies the implementation of these models. If risk aversion is time-varying, but incorrectly assumed to be constant, then this can induce large pricing errors because the misspecified model leads to an incorrect option pricing formula. The assumption of constant risk aversion is contradicted by empirical evidence, and several theoretical models with time-varying risk aversion have been proposed in the literature, see e.g. Campbell and Cochrane (1999), Li (2007), Chabi-Yo et al. (2008), and Bekaert et al. (2021).

In this paper, we propose a novel state-dependent pricing kernel with a variance risk premium and time-varying risk aversion. First, we introduce a new discrete-time volatility model within the Realized GARCH framework of Hansen et al. (2012), in which a latent state follows a *hidden* Markov switching process. The same Markov switching process is used to introduce time-variation in the pricing kernel, and this leads to a pricing kernel with a state-dependent variance risk premium. The framework has a great deal of flexibility in terms of the statistical model for the observed variables under $\mathbb{P}$ and in terms of the plasticity of the pricing kernel. It is, nevertheless, possible to derive the corresponding pricing formula for European options by means of an analytical approximation method. The Markov-switching Realized GARCH model is relatively simple to estimate by quasi maximum likelihood, and the latent states can be inferred from the observed realized volatility measures and returns. The Realized GARCH framework is well suited for this problem because a key component in the model is a volatility-specific shock. This shock is inferred from the difference between the realized volatility measure and its conditional expectation, and it can be incorporated in the pricing kernel to include a variance risk premium.[3] Estimation that includes the estimation of the parameters in the pricing kernel is more involved because it relies on the observed option prices.[4]

In this paper, we conduct an extensive empirical analysis with a large panel of S&P 500 index

[2] An inverse S-shaped implies that investors tend to overweight low-probability events while they underweight the likelihood of events with high probability. The opposite is true with a regular S-shape.

[3] A growing literature is exploring ways to utilize realized volatility measures for derivatives pricing, see e.g. Corsi et al. (2013); Christoffersen et al. (2014); Majewski et al. (2015); Huang et al. (2017, 2019); Tong and Huang (2021).

[4] Hansen and Tong (2021) also introduces an option pricing model with time-varying volatility risk aversion. Their framework is different in two important ways. First, they build on the Heston-Nandi GARCH model (Heston and Nandi, 2000). Second, they use a score-driven model, see Creal et al. (2013), to model time-variation in risk aversion.

option prices based on 30 years of data (from 1990 to 2019). We find the volatility risk aversion to be time-varying. Investors tend to be more risk-averse during periods with high volatility, but there are also periods where investors have a slight appetite for the variance risk, such as during the low-volatility periods: 1993-1995, 2004-2007, and 2014-2017. This is consistent with other studies that report a positive volatility risk premium during these periods. On average, we find the volatility risk premium to be negative, which is consistent with existing literature. In terms of option pricing performance, our empirical results show that the proposed framework outperforms other benchmarks by reducing option pricing errors by 15% or more. These reductions in pricing errors are found both in-sample and out-of-sample.

The successful fusion of a GARCH model with a Markov switching structure is an accomplishment that deserves some commenting. Estimation of GARCH models with Markov switching is typically marred with complications. For instance, the path-dependence problem makes it nearly impossible to evaluate the sample likelihood function. The solution by Cai (1994) and Hamilton and Susmel (1994) is only valid within an ARCH specification. Other approaches, such as those by Gray (1996), and Klaassen (2002), are not suitable for asset pricing due to the difficulties in risk neutralization.[5] Chen and Hung (2010) directly assume a Markov-switching GARCH process for returns under the risk-neutral measure and obtain option prices by a lattice method, volatility discretization, and Monte Carlo simulation. However, their model is not amenable to estimation and the authors resort to calibration instead. Elliott et al. (2006) develop a method for a Heston-Nandi GARCH model with Markov switching, but it requires the Markov states to be observable. For this reason, there is not much empirical literature on option pricing based on a GARCH model with a hidden Markov switching structure.[6]

The key to our successful coupling of a hidden Markov switching model with a GARCH-type model is the presence of the realized measures of volatility in the model. By providing accurate information about the contemporaneous volatility level, the realized measure adds valuable information about the latent state, and the Realized GARCH model maintains the structure that permits straightforward estimation based on returns and realized measures. The most complicated part of the framework relates to the analytical approximation for option pricing, because it requires many terms to be computed. The expressions for these terms are computed in the Appendix and are

[5] Most option pricing models under the specification of Gray (1996) are constructed without specifying risk premium, see e.g. Satoyoshi and Mitsui (2011) and Daouk and Guo (2004).

[6] There are several Markov switching models for option pricing without GARCH structures, see e.g. Duan et al. (2002), Aingworth et al. (2006), Liew and Siu (2010), and Shen et al. (2014).

plugged into the generic expressions derived in Duan et al. (1999, p. 104).

The rest of the paper is organized as follows. In Section 2, we propose the theoretical model under the physical measure, $\mathbb{P}$, the risk neutralization process under a state-dependent pricing kernel, and details about the estimation of the Markov switching Realized GARCH model. Section 3 introduces the analytical approximation formula for European call options. Section 4 presents the competing models used in our empirical comparisons. Section 5 describes the joint estimation method. All empirical results are presented in Section 6 including the summary statistics, parameters estimation, and in-sample and out-of-sample option pricing performance. All relevant proofs are presented in Appendix A, and Appendix B derives the terms needed for option pricing.

2 The Model

Let $\mathscr{F}_t = \sigma(\{R_\tau, x_\tau\}, \tau \leq t)$ denote the natural filtration, where $R_{t+1} = \log(S_{t+1}/S_t)$ is the daily log-return, and x_t is the realized measure of volatility. The latter is, in our empirical analysis, computed from high-frequency data with the Realized Kernel by Barndorff-Nielsen et al. (2008).

2.1 The Realized GARCH Model ($\mathbb{P}$),

The Realized GARCH framework was introduced by Hansen et al. (2012). In this paper, we build on the variant proposed in Hansen and Huang (2016) that was also used for option pricing in Huang et al. (2017). The dynamic properties of returns, the conditional variance, $h_{t+1} = \text{var}(R_{t+1}|\mathscr{F}_t)$, and the realized volatility measure are given by the equations:

$$
\begin{aligned}
R_{t+1} &= r + \lambda\sqrt{h_{t+1}} - \tfrac{1}{2}h_{t+1} + \sqrt{h_{t+1}}z_{t+1}, && (1)\\
\log h_{t+1} &= \omega + \beta\log h_t + \gamma\log x_t + \tau_1 z_t + \tau_2(z_t^2 - 1), && (2)\\
\log x_t &= \xi + \phi\log h_t + \delta_1 z_t + \delta_2(z_t^2 - 1) + \sigma u_t. && (3)
\end{aligned}
$$

The intercept in the return equation, r, denotes the risk-free rate and λ is the equity risk premium. The stochastic properties are driven by two i.i.d standard normally distributed "innovations", z_t and u_t, that represent return and volatility shocks, respectively.

Realized GARCH models are characterized by the measurement equation, (3), that defines the relationship between the conditional variance, h_t, and the realized measure x_t. Unlike the conventional GARCH model, this model has two distinct innovations, z_t and u_t, where the second is

similar to the random innovation for volatility in stochastic volatility models. However, because the Realized GARCH model is an observation-driven model, it is simpler to estimate than stochastic volatility models. For the purpose of derivative pricing, the Realized GARCH structure is especially valuable because the two innovation terms can be used as risk factors, as we explore below.

2.2 The Markov-switching Realized GARCH Model ($\mathbb{P}$)

Here, we introduce a new volatility model based on the Realized GARCH model above. Specifically, we will introduce time-variation in the intercept of the measurement equation, ξ, by assuming it is driven by a hidden Markov process, $\{s_t\}$. One may think of the states as representing different market conditions. We refer to this model as the Markov-switching Realized GARCH model. We assume that the state variable, $s_t \in \{e_1, \ldots, e_N\}$, follows a stationary discrete-time hidden Markov chain process on $(\Omega, \mathscr{G}, \mathbb{P})$, with transition probabilities, $\pi_{ij} \equiv \Pr(s_{t+1} = e_j | s_t = e_i)$, $i, j = 1, \ldots, N$. So, the Markov-switching Realized GARCH model is given by (1), (2), and a state-dependent measurement equation:

$$\log x_t = \xi_{s_t} + \phi \log h_t + \delta_1 z_t + \delta_2 (z_t^2 - 1) + \sigma u_t. \tag{3'}$$

The conventional Realized GARCH model corresponds to the case with a single state ($N = 1$). We can, without loss of generality, represent the states by the N unit vectors, i.e. let e_j be the j-th column of the $N \times N$ identity matrix I_N. With this convention we have $\xi_{s_t} = \xi' s_t$, where $\xi \in \mathbb{R}^{N \times 1}$ is a vector of parameters with $\xi_j \equiv \xi_{(s_t = e_j)}$, $j = 1, \ldots, N$. Note that the parameter ξ_j controls the long-run volatility level within each state because the dynamic properties of $\log h_t$ are given by:

$$\log h_{t+1} = \omega + \gamma \xi' s_t + (\beta + \gamma\phi) \log h_t + (\tau_1 + \gamma\delta_1) z_t + (\tau_2 + \gamma\delta_2)(z_t^2 - 1) + \gamma\sigma u_t.$$

Thus, if $|\beta + \gamma\phi| < 1$, then $\log h_t$ is mean-reverting towards $(\omega + \gamma\xi_j)/(1 - \beta - \gamma\phi)$ in the j-th state, $j = 1, \ldots, N$. Thus, the Markov switching model for ξ is effectively a Markov switching model for the long-run level of volatility. This highlights the motivations for introducing time-variation in this parameter. Another advantage of mapping states to the measurement equation is that inference about states can be simply inferred from the realized measures and returns. Introducing Markov switching in other parameters would greatly complicate the analysis and, in some cases, make analytical option pricing formulae unobtainable.

2.3 Risk Neutralization ($\mathbb{Q}$)

Next, we turn to the risk neutralization as characterized by the pricing kernel. For this purpose, we generalized the exponentially affine pricing kernel

$$M_{t+1,t} = \frac{\exp[\psi z_{t+1} + \chi u_{t+1}]}{\mathbb{E}_t^{\mathbb{P}}[\exp(\psi z_{t+1} + \chi u_{t+1})]},$$

to be state-dependent. Here $\mathbb{E}_t^{\mathbb{P}}(\cdot) \equiv \mathbb{E}^{\mathbb{P}}(\cdot|\mathscr{F}_t)$. This kernel was introduced within the Realized GARCH framework by Huang et al. (2017), where the parameters, ψ and χ, govern the equity risk premium and the variance risk premium, respectively. We generalize this pricing kernel by substituting ψ_{s_t} for ψ and χ_{s_t} for χ. However, it immediately follows that the former must be constant, because a no-arbitrage condition has the implication that $\psi_{s_t} = -\lambda$, which rules out time-variation in ψ, see Appendix A.1. Thus, the time-variation across states is confined to that in χ_{s_t}, and our state-dependent pricing kernel is given by:

$$M_{t+1,t}(s_{t+1}) = \frac{\exp(\psi z_{t+1} + \chi_{s_{t+1}} u_{t+1})}{\mathbb{E}_t^{\mathbb{P}}[\exp(\psi z_{t+1} + \chi_{s_{t+1}} u_{t+1})|s_{t+1}]}. \tag{4}$$

Note that the additional conditioning on s_{t+1} is required due to the additional source of uncertainty induced by the hidden regime-switching part of the model. The appropriate martingale condition is, therefore, given by the enlarged filtration: $\mathscr{G}_{t+1} \vee \mathscr{F}_t$, where $\mathscr{G}_t = \sigma(\{s_\tau\}, \tau \leq t)$. Naturally, by the law of iterated expectations it follows that the martingale condition holds with $\mathscr{F}_t$ alone, if it holds for the enlarged filtration. And $\mathscr{F}_t$ conveniently does not require knowledge about the latent state. The dynamic properties under the risk-neutral measure, $\mathbb{Q}$, are as stated in the following theorem.

Theorem 1. *Suppose that returns and realized volatilities under the $\mathbb{P}$-measure follow the Markov-switching Realized GARCH model in (1), (2), (3'), and the pricing kernel is given by (4). Then, under $\mathbb{Q}$, we have that $z_{t+1}^* \equiv z_{t+1} + \lambda$ and $u_{t+1}^* \equiv u_{t+1} - \chi_{s_{t+1}}$ are independent and identically distributed, $N(0,1)$, and*

$$\begin{aligned}
R_{t+1} &= r - \tfrac{1}{2} h_{t+1} + \sqrt{h_{t+1}} z_{t+1}^*, \\
\log h_{t+1} &= \omega^* + \beta \log h_t + \gamma \log x_t + \tau_1^* z_t^* + \tau_2 (z_t^{*2} - 1), \\
\log x_t &= \xi_{s_t}^* + \phi \log h_t + \delta_1^* z_t^* + \delta_2 (z_t^{*2} - 1) + \sigma u_t^*,
\end{aligned}$$

where $\omega^* = \omega - \tau_1\lambda + \tau_2\lambda^2$, $\tau_1^* = \tau_1 - 2\tau_2\lambda$, $\delta_1^* = \delta_1 - 2\delta_2\lambda$ *and*

$$\xi_{s_t}^* = \xi_{s_t} - \delta_1\lambda + \delta_2\lambda^2 + \sigma\chi_{s_t}.$$

We seek to characterize the implications of a state-dependent variance risk premium parameter, χ_{s_t}. To this end, we consider the difference between conditional expectations of log-variance under $\mathbb{P}$ and under $\mathbb{Q}$,

$$\mathbb{E}_t^{\mathbb{Q}}(\log h_{t+2}) - \mathbb{E}_t^{\mathbb{P}}(\log h_{t+2}) = -\left(\tau_1 + \gamma\delta_1\right)\lambda + \left(\tau_2 + \gamma\delta_2\right)\lambda^2 + \gamma\sigma\mathbb{E}_t^{\mathbb{P}}(\chi_{s_{t+1}}), \tag{5}$$

which is a logarithmic variant of the variance risk premium. This quantity can be decomposed into compensation for equity risk and additional compensation for volatility risk. The former is given by the first two terms in (5), which involve λ, and the latter is the last term in (5), which is state-dependent. Thus, the parameter χ_{s_t} governs the variance risk aversion of investors in state s_t, where a large value of χ is associated with a high variance risk premium.

Note that the expectation $\mathbb{E}_t^{\mathbb{P}}(\chi_{s_{t+1}})$ can be also expressed as $\sum_{s_{t+1}} P_t(s_{t+1})\chi_{s_{t+1}}$, where $P_t(s_{t+1})$ is the notation for the conditional distribution $\Pr(s_{t+1}|\mathscr{F}_t)$, over the possible states, $e_1,\ldots,e_N$. Similarly, we use $P_t(s_t)$ as compact notation for $\Pr(s_t|\mathscr{F}_t)$. Next, we will derive model-based expressions for multi-step ahead forecasts of h_t, which defines the, so-called, *variance term structure*.

Corollary 1. *The model-implied n-periods ahead forecast of* h_t *within the Markov-switching Realized GARCH model under* $\mathbb{Q}$ *is:*

$$\mathbb{E}_t^{\mathbb{Q}}(h_{t+n}|s_t) = \exp\left(\kappa_n + \rho^{n-1}\log h_{t+1} + \theta_n' s_t\right), \tag{6}$$

with $\rho = \beta + \gamma\phi$. *The vector* $\theta_n \in \mathbb{R}^{N\times 1}$ *is given recursively from,*

$$\theta_{n+1} = \Delta\left(\rho^{n-1}\zeta + \theta_n\right), \quad \Delta_i(\varphi) \equiv \log\left[\sum_{j=1}^{N}\pi_{ij}\exp(\varphi_j)\right],$$

with initial condition $\theta_1 = \mathbf{0}$, *and* $\zeta_j = \omega^* + \gamma\xi_j^*$, $j = 1,\ldots,N$. *The intercept term is given by* $\kappa_n = \sum_{i=0}^{n-2} G(\rho^i)$, *where the function* $G(\cdot)$ *is the logarithm of the moment generating function (MGF) for the random variable* $(\tau_1^* + \gamma\delta_1^*)z_t^* + (\tau_2 + \gamma\delta_2)(z_t^{*2} - 1) + \gamma\sigma u_t^*$.

Corollary 1 shows that the variance term structure, $\mathbb{E}_t^{\mathbb{Q}}(h_{t+n}|s_t)$, for $n = 1,2,\ldots$, depends on the current state s_t and the current level of volatility, h_{t+1}, where the latter is $\mathscr{F}_t$-measurable. A major

benefit of having a closed-from expression for $\mathbb{E}_t^{\mathbb{Q}}(h_{t+n}|s_t)$ is that it leads to an analytical expression for the model-implied VIX price. In the present context, the VIX pricing formula is given by

$$\text{VIX}_t = A \times \sqrt{\sum_{n=1}^{22} \mathbb{E}_t^{\mathbb{Q}}(h_{t+n})} = A \times \sqrt{\sum_{n=1}^{22} \sum_{j=1}^{N} \mathbb{E}_t^{\mathbb{Q}}(h_{t+n}|s_t) P_t(s_t = e_j)},$$

where $A = 100\sqrt{252/22}$ is the annualized factor.

2.4 Model Estimation by Maximum Likelihood ($\mathbb{P}$)

In this section, we discuss the estimation of the Markov-switching Realized GARCH model based on returns and realized measures alone. In Section 5, we will discuss how option prices can be incorporated in the estimation of this model in conjunction with the parameters in the pricing kernel.

The model is relatively simple to estimate by maximum likelihood for $\{(R_t, x_t)\}_{t=1}^T$. The likelihood for (R_{t+1}, x_{t+1}) is given by their density, conditional on $\mathscr{F}_t$, $L_t(R_{t+1}, x_{t+1}) = f(R_{t+1}, x_{t+1}|\mathscr{F}_t)$, which we can rewrite as

$$\begin{aligned} L_t(R_{t+1}, x_{t+1}) &= \sum_{s_{t+1}} P_t(s_{t+1}) L_t(R_{t+1}, x_{t+1}|s_{t+1}) \\ &= \sum_{s_{t+1}} P_t(s_{t+1}) L_t(R_{t+1}|s_{t+1}) L_t(x_{t+1}|R_{t+1}, s_{t+1}) \\ &= \sum_{s_{t+1}} P_t(s_{t+1}) L_t(R_{t+1}) L_t(x_{t+1}|R_{t+1}, s_{t+1}). \end{aligned} \tag{7}$$

The last equality uses that the distribution of $R_{t+1} = r + \lambda\sqrt{h_{t+1}} - \frac{1}{2}h_{t+1} + \sqrt{h_{t+1}}z_{t+1}$, conditional on $\mathscr{F}_t$, does not depend on the state, s_{t+1}. The reason is that h_{t+1} is $\mathscr{F}_t$-measurable and z_{t+1} is independent of s_{t+1}, such that $L_t(R_{t+1}|s_{t+1}) = L_t(R_{t+1})$. This term of the likelihood function is

$$L_t(R_{t+1}) = \frac{1}{\sqrt{2\pi h_{t+1}}} \exp\left\{ -\frac{1}{2} \frac{[R_{t+1} - (r + \lambda\sqrt{h_{t+1}} - h_{t+1}/2)]^2}{h_{t+1}} \right\}.$$

Next, the conditional distribution of the realized measure, $L_t(x_{t+1}|R_{t+1}, s_{t+1})$, is log-normally distributed. From the measurement equation, (3'), and the Gaussian specification, we have

$$L_t(x_{t+1}|R_{t+1}, s_{t+1}) = \frac{1}{\sqrt{2\pi\sigma^2}} \exp\left\{ -\frac{1}{2} \frac{[x_{t+1} - (\xi_{s_{t+1}} + \phi \log h_{t+1} + \delta_1 z_{t+1} + \delta_2(z_{t+1}^2 - 1))]^2}{\sigma^2} \right\}.$$

Finally, the remaining term in (7), $P_t(s_{t+1})$, is the conditional state distribution. The relation between

$P_t(s_{t+1})$ and $P_t(s_t)$ is given by

$$P_t(s_{t+1}) = \sum_{s_t} P_t(s_{t+1}|s_t)P_t(s_t) = \sum_{s_t} P(s_{t+1}|s_t)P_t(s_t), \tag{8}$$

where the last equality follows by the transition probabilities being time-invariant and independent of $\{R_t, x_t\}$. Before we can evaluate (7), we need to compute $P_t(s_t)$. From Bayes' Theorem we have,

$$\Pr(s_t|R_t, x_t, \mathscr{F}_{t-1}) = \frac{\Pr(R_t, x_t, s_t|\mathscr{F}_{t-1})}{\Pr(R_t, x_t|\mathscr{F}_{t-1})} = \frac{\Pr(R_t, x_t|s_t, \mathscr{F}_{t-1})\Pr(s_t|\mathscr{F}_{t-1})}{\Pr(R_t, x_t|\mathscr{F}_{t-1})},$$

where the first term is identical to $P_t(s_t)$ and the last is identical to $\frac{L_{t-1}(R_t,x_t|s_t)P_{t-1}(s_t)}{L_{t-1}(R_t,x_t)}$. So,

$$\begin{aligned} P_t(s_t) &= \frac{L_{t-1}(R_t, x_t|s_t)P_{t-1}(s_t)}{L_{t-1}(R_t, x_t)} = \frac{L_{t-1}(R_t, x_t|s_t)P_{t-1}(s_t)}{\sum_{s'_t} L_{t-1}(R_t, x_t|s'_t)P_{t-1}(s'_t)} \\ &= \frac{L_{t-1}(R_t)L_{t-1}(x_t|R_t, s_t)P_{t-1}(s_t)}{\sum_{s'_t} L_{t-1}(R_t)L_{t-1}(x_t|R_t, s'_t)P_{t-1}(s'_t)} = \frac{L_{t-1}(x_t|R_t, s_t)P_{t-1}(s_t)}{\sum_{s'_t} L_{t-1}(x_t|R_t, s'_t)P_{t-1}(s'_t)}. \end{aligned} \tag{9}$$

In the third equality, we used that $L_{t-1}(R_t|s_t) = L_{t-1}(R_t)$. By combining (8) and (9), we arrive at the following recursive formula for $P_t(s_{t+1})$:

$$P_t(s_{t+1}) = \frac{\sum_{s_t} \pi_{s_t,s_{t+1}} L_{t-1}(x_t|R_t, s_t)P_{t-1}(s_t)}{\sum_{s'_t} L_{t-1}(x_t|R_t, s'_t)P_{t-1}(s'_t)}, \tag{10}$$

that defines the recursion from $P_{t-1}(s_t)$ to $P_t(s_{t+1})$. Therefore, given an initial value for $P_0(s_1)$, we can evaluate the likelihood function for $\{(R_t, x_t)\}_{t=1}^T$. There are two obvious ways to obtain an initial value for $P_0(s_1)$. One can either model it as an unknown vector (of conditional state probabilities) to be estimated, or one can assign $P_0(s_1)$ to have its stationary distribution, which is given by the eigenvector, $\pi'\Pi = \pi'$. In our empirical implementation, we use the latter.

The recursion for state probabilities, (10), depends on the conditional distribution of realized measures, but does not depend on the conditional distribution for returns. The reason is that the state, s_t, only impacts the intercept in the measurement equation. The recursive expression for state probabilities, (10), also holds when option prices are included in the analysis and parameters are estimated by maximization of the total likelihood. However, the joint estimation will influence all parameter estimates, which will influence the likelihood for the realized measure, $L_{t-1}(x_t|R_t, s_t)$. Thus, the estimated state probabilities based on $\{(R_t, x_t)\}_{t=1}^T$, need not be identical to those obtained from joint estimation that also includes option prices.

3 Analytical Approximation for European Call Options

The properties of the model under the $\mathbb{Q}$-measure were presented in Theorem 1, and it is evident that there is no analytical formula for the moment generating function (MGF) of cumulative return. This complication is not a consequence of the Markov switching structure because the complication is also present without Markov switching ($N = 1$). Without an analytical formula for the MGF, the conventional path to closed-form pricing expressions with Fourier inversion is not applicable. Instead, we follow the method developed in Huang et al. (2017) and derive an analytical approximation based on an Edgeworth expansion of the density for the cumulative return.

The European call option price is given by

$$C_t = e^{-r(T-t)}\mathbb{E}_t^{\mathbb{Q}}\left(\max\left(S_T - K, 0\right)\right) = \sum_{s_t} P_t(s_t) C_t(s_t),$$

where $C_t(s_t) \equiv e^{-r(T-t)}\mathbb{E}_t^{\mathbb{Q}}\left(\max\left(S_T - K, 0\right)|s_t\right)$, T is the date of maturity, S_T is the terminal stock price, and K is the strike price. Let $R_T = \log(S_T/S_t)$ be the future cumulated return, $\mu = \mathbb{E}_t^{\mathbb{Q}}(R_T|s_t)$, and $\sigma^2 = \mathrm{Var}_t^{\mathbb{Q}}\left(R_T|s_t\right)$, then the expectation can be written as an integral of the standardized cumulated return $z_T = \left(R_T - \mu\right)/\sigma$:

$$C_t(s_t) = e^{-r(T-t)} \int_{-\infty}^{k} \left[S_t \exp(\mu - \sigma z) - K\right] \tilde{g}(z) \mathrm{d}z,$$

where $k = \left(\log\left(S_t/K\right) + \mu\right)/\sigma$ and $\tilde{g}(z)$ is the true conditional density function of $-z_T$ given s_t. Following Jarrow and Rudd (1982), we apply a second-order Edgeworth expansion by expanding the density of the standardized cumulated return, z_T, using the expression,

$$\tilde{g}(z) \approx \left[1 - \frac{\kappa_3}{6} H_3(z) + \frac{(\kappa_4 - 3)}{24} H_4(z) + \frac{\kappa_3^2}{72} H_6(z)\right] \phi(z). \tag{11}$$

Here $\phi(z) = (2\pi)^{-\frac{1}{2}} \exp(-z^2/2)$ is the density of the standard normal distribution, $\kappa_3 = \mathbb{E}_t^{\mathbb{Q}}(z_T^3|s_t)$, $\kappa_4 = \mathbb{E}_t^{\mathbb{Q}}(z_T^4|s_t)$, and $H_n(z)$ is the n-th order Hermite polynomial given by

$$H_3(z) = z^3 - 3z, \qquad H_4(z) = z^4 - 6z^2 + 3, \quad \text{and} \quad H_6(z) = z^6 - 15z^4 + 45z^2 - 15.$$

From Huang et al. (2017, proposition 1), the price of a European call option is approximated by

$$C_t(s_t) \approx A_0 + \frac{\kappa_3}{6}A_3 + \frac{(\kappa_4 - 3)}{24}A_4 + \frac{\kappa_3^2}{72}A_6, \tag{12}$$

where

$$\begin{aligned}
A_0 &= S_t e^{\delta\sigma}\Phi(d) - Ke^{-r(T-t)}\Phi(d-\sigma), \\
A_3 &= S_t e^{\delta\sigma}\sigma\left[(2\sigma - d)\phi(d) + \sigma^2\Phi(d)\right], \\
A_4 &= S_t e^{\delta\sigma}\sigma\left[\left(d^2 - 1 - 3\sigma(d-\sigma)\right)\phi(d) + \sigma^3\Phi(d)\right], \\
A_6 &= S_t e^{\delta\sigma}\sigma\left[\sigma^5\Phi(d) + \left(3 - 6d^2 + d^4 + 5\sigma\left(d - (d-\sigma)(\sigma d - 2) - (d-\sigma)^3\right)\right)\phi(d)\right], \\
d &= \frac{\log(S_t/K) + \mu}{\sigma} + \sigma.
\end{aligned}$$

Before we can obtain options prices with (12), we need to derive the third and fourth moments of the standardized cumulative return, z_T,

$$\kappa_3 = \frac{1}{\sigma^3}\left[\mathbb{E}_t^{\mathbb{Q}}\left(R_T^3|s_t\right) - \mu^3\right] - 3\frac{\mu}{\sigma}, \quad \text{and} \quad \kappa_4 = \frac{1}{\sigma^4}\left[\mathbb{E}_t^{\mathbb{Q}}\left(R_T^4|s_t\right) - \mu^4\right] - 2\frac{\mu}{\sigma}\left(2\kappa_3 + 3\frac{\mu}{\sigma}\right).$$

The remaining problem is to obtain expressions for $\mathbb{E}_t^{\mathbb{Q}}(R_T^3|s_t)$ and $\mathbb{E}_t^{\mathbb{Q}}(R_T^4|s_t)$. These expressions involve a large number of terms, which are derived in Appendix B.

In Figure 1, we present the approximated density for z_T (under $\mathbb{Q}$) and the true density. The latter is simulated from the model we estimated in our empirical application, see Table 2. The model has two states, and the densities are for the standardized cumulative return, z_T, over six months in the high-volatility state. The red solid line is the approximated risk-neutral distribution and the blue line is the "true" risk-neutral distribution for z_T. The latter was obtained with 100,000 simulations. The approximation method largely agrees with the true density.

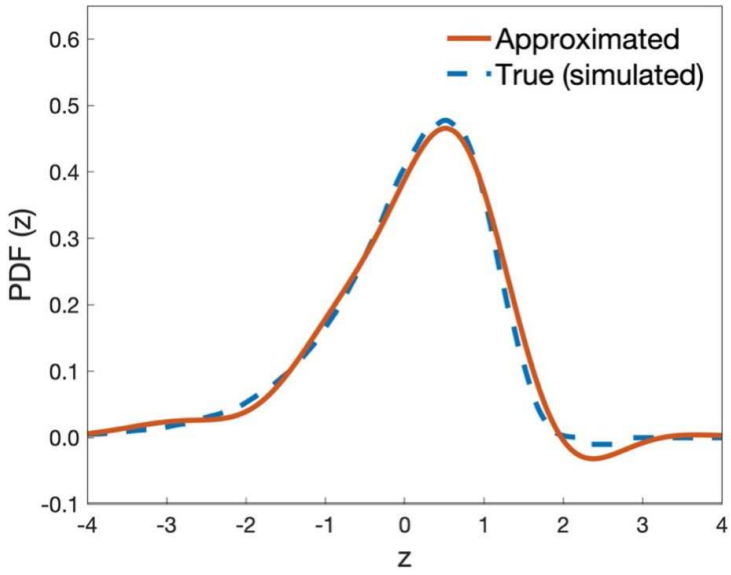


Figure 1: The approximate risk-neutral distribution of standardized cumulated return, z_T, over six months for the Markov-switching Realized GARCH model based on the Edgeworth expansion (red solid line) and the true density (blue dashed line). The true density is obtained by 100,000 simulations, using a design based on the estimated parameters in Table 2.

4 Model Comparison

We compare the newly proposed Markov-switching Realized GARCH model (denote MS-RG) to several existing models, including a range of models that have documented the benefit of incorporating realized measures into discrete-time option pricing models. We also include the variant of the Realized GARCH model by Huang et al. (2017) (denote RG), which is nested in our framework as the case $N = 1$.

4.1 GARV

The Generalized Affine Realized Volatility (GARV) model was proposed by Christoffersen et al. (2014). This model assumes that the conditional variance for returns, $\bar{h}_t$, has two components. The first, h_t^R, is driven by returns, and the second, h_t^{RV}, is driven by the realized measure (RV). This

model takes the form:

$$\begin{aligned}
R_{t+1} &= r+(\lambda-\tfrac{1}{2})\bar{h}_{t+1}+\sqrt{\bar{h}_{t+1}}z_{t+1},\\
\bar{h}_{t+1} &= \xi h^R_{t+1}+(1-\xi)h^{\mathrm{RV}}_{t+1},\\
h^R_{t+1} &= \omega+\beta h^R_t+\tau_2(z_t-\tau_1\sqrt{\bar{h}_t})^2,\\
h^{\mathrm{RV}}_{t+1} &= \kappa+\phi h^{\mathrm{RV}}_t+\delta_2(\varepsilon_t-\delta_1\sqrt{\bar{h}_t})^2,\\
\mathrm{RV}_t &= h^{\mathrm{RV}}_t+\vartheta(\varepsilon^2_t-1-2\delta_1\varepsilon_t\sqrt{\bar{h}_t}),
\end{aligned}$$

where (z_t,ε_t) follows a standard bivariate normal distribution with a correlation of ρ. The dynamic properties under $\mathbb{Q}$ can be obtained through $z^*_t=z_t+\lambda\sqrt{\bar{h}_t}$ and $\varepsilon^*_t=\varepsilon_t+\chi\sqrt{\bar{h}_t}$, where (z^*_t,ε^*_t) also follows a standard bivariate normal distribution with correlation ρ. As in the Realized GARCH model, the parameter χ is associated with the variance risk premium, and a positive χ implies a negative variance risk premium.[7] Due to the affine structure of the GARV model, a closed-form option price is available.

4.2 LHARG

In addition to GARCH-type models, the availability of high-frequency data and realized measures has boosted the development of reduced-form models such as the HAR model. In particular, the HAR model was adapted by using the leverage function of the Heston-Nandi GARCH as well as a noncentral gamma distribution (LHARG) to price European call options. Majewski et al. (2015) provided a general framework for option pricing with an LHARG model.

$$R_{t+1}=r+(\lambda-\tfrac{1}{2})\mathrm{RV}_{t+1}+\sqrt{\mathrm{RV}_{t+1}}z_{t+1},\quad \mathrm{RV}_{t+1}|\mathscr{F}_t\sim\Gamma(\delta,\Theta_t,\theta),$$

$$\Theta_t\theta=d+\beta_d\mathrm{RV}^{(d)}_t+\beta_w\mathrm{RV}^{(w)}_t+\beta_m\mathrm{RV}^{(m)}_t+\alpha_d\bar{\ell}^{(d)}_t+\alpha_w\bar{\ell}^{(w)}_t+\alpha_m\bar{\ell}^{(m)}_t,$$

$$\begin{aligned}
\mathrm{RV}^{(d)}_t &= \mathrm{RV}_t, & \ell^{(d)}_t &= \left(z^2_t-1-2\gamma z_t\sqrt{\mathrm{RV}_t}\right),\\
\mathrm{RV}^{(w)}_t &= \frac{1}{4}\sum_{i=1}^{4}\mathrm{RV}_{t-i}, & \ell^{(w)}_t &= \frac{1}{4}\sum_{i=1}^{4}\left(z^2_{t-i}-1-2\gamma z_{t-i}\sqrt{\mathrm{RV}_{t-i}}\right),\\
\mathrm{RV}^{(m)}_t &= \frac{1}{17}\sum_{i=5}^{21}\mathrm{RV}_{t-i}, & \ell^{(m)}_t &= \frac{1}{17}\sum_{i=5}^{21}\left(z^2_{t-i}-1-2\gamma z_{t-i}\sqrt{\mathrm{RV}_{t-i}}\right).
\end{aligned}$$

[7] We report $\gamma=\delta_2/\vartheta$ instead of ϑ because the former can be used to measure the contribution of the realized information to the volatility process.

Majewski et al. (2015) denoted this model by ZM-LHARG due to the zero-mean leverage function. They found it has the best option pricing performance because its less-constrained leverage allows the process to explain a larger fraction of the skewness and kurtosis observed in real data. The risk-neutral dynamics are given by:

$$R_{t+1} = r - \tfrac{1}{2}\mathrm{RV}_{t+1} + \sqrt{\mathrm{RV}_{t+1}}z^*_{t+1}, \quad \mathrm{RV}_{t+1}|\mathscr{F}_t \sim \Gamma(\delta, \Theta^*_t, \theta^*),$$

where $z^*_t = z_t + \lambda\sqrt{\mathrm{RV}_t}$ follows a standard normal distribution. The risk-neutral parameters are linked to the physical parameters as follows:

$$\Theta^*_t = \chi\Theta_t,\ \theta^* = \chi\theta,\ d^* = \chi^2 d,\ \beta^*_j = \chi^2(\beta_j + \alpha_j\left((\gamma+\lambda)^2 - \gamma^2\right)),\ \alpha^*_j = \chi^2\alpha_j,\ \text{for } j \in \{d,w,m\},$$

where $\chi = (1 + \theta(\frac{1}{2}(\lambda - \frac{1}{2})^2 - v_0 - \frac{1}{8}))^{-\frac{1}{2}}$. Here, a negative v_0 is associated with a negative variance risk premium. Majewski et al. (2015) derive the option-pricing formula for this model.

4.3 Heston–Nandi GARCH model

The last competing model is the Heston–Nandi GARCH model (hereafter HNG) presented by Heston and Nandi (2000). HNG is one of very few discrete-time volatility models that yield an analytical option pricing formula. We adopt the variance dependent pricing kernel introduced in Christoffersen et al. (2013) to risk neutralize the HNG model, which takes the variance premium into account. The dynamic properties under the physical measures are given by

$$\begin{aligned} R_{t+1} &= r + (\lambda - \tfrac{1}{2})h_{t+1} + \sqrt{h_{t+1}}z_{t+1}, \\ h_{t+1} &= \omega + \beta h_t + \tau_2\left(z_t - \tau_1\sqrt{h_t}\right)^2. \end{aligned}$$

The corresponding risk-neutral dynamics with the variance-augmented pricing kernel are given by:

$$\begin{aligned} R_{t+1} &= r - \tfrac{1}{2}h^*_{t+1} + \sqrt{h^*_{t+1}}z^*_{t+1}, \\ h^*_{t+1} &= \omega^* + \beta h^*_t + \tau^*_2\left(z^*_t - \tau^*_1\sqrt{h^*_t}\right)^2, \end{aligned}$$

where z^*_{t+1} has a standard normal distribution and the risk-neutral parameters are

$$h^*_t = \chi h_t, \quad \omega^* = \chi\omega, \quad \tau^*_2 = \chi^2\tau_1 \quad \tau^*_1 = \left(\lambda + \tau_1 - \frac{1}{2}\right)\chi^{-1} + \frac{1}{2}.$$

Once again, the parameter χ is associated with the variance risk premium, where $\chi > 1$ corresponds to negative variance risk premium.

5 Estimation Method

In this section, we turn to model estimation including the pricing kernel. In Section 2.4 we estimated the Markov-switching Realized GARCH model from $\{(R_t, x_t)\}_{t=1}^T$ alone. Now, we will include option prices in estimation, and simultaneously estimate parameters in the pricing kernel and the parameters in the Markov-switching Realized GARCH model. We adopt the quasi log-likelihood for the option prices from Christoffersen et al. (2013) and combine it with the log-likelihood for $\{(R_t, x_t)\}_{t=1}^T$. The quasi log-likelihood function for option prices by Christoffersen et al. (2013) assumes that option pricing errors, measured in units of the Black-Scholes Vega-units,

$$e_i = \frac{O_i^{\text{Model}} - O_i^{\text{Market}}}{v_i^{bs}}, \qquad i = 1, \dots, N,$$

are normally distributed, $e_i \sim iidN(0, \sigma_e^2)$. Here, O_i^{Model} and O_i^{Market} represent the model-implied option price and the observed market-based option price, respectively, v_i^{bs} is the corresponding Black-Scholes Vega, and N is the total number of option prices in the sample period. The Vega-weighted pricing error mimics the difference in the implied volatilities, and σ_e^2 denotes the variance of the Vega-weighted pricing errors.

Parameters are estimated by maximizing the total quasi log-likelihood function, $\ell_{\text{Total}} = \ell_{R,x} + \ell_o$, where the expression of $\ell_{R,x}$ is given in Section 2.4, and ℓ_o is

$$\ell_o \quad = \quad \left\{ -\frac{N}{2}\log(2\pi) - \frac{1}{2}\sum_{i=1}^{N}\log(\sigma_e^2) - \sum_{i=1}^{N}\frac{1}{2\sigma_e^2}\left(O_i^{\text{Model}} - O_i^{\text{Market}})/v_i^{bs}\right)^2 \right\} \times \frac{T}{N}.$$

In the inclusion of the quasi log-likelihood for option prices, we follow Christoffersen et al. (2012), Ornthanalai (2014), and Huang et al. (2019), and scale ℓ_o by $\frac{T}{N}$. This amounts to an adjustment for the imbalance between the number of observed option prices and the number of observation of (R_t, x_t), which serves to prevent that parameter estimation is largely dominated by the option data.

6 Empirical Results

6.1 Data

Our empirical analysis is based on close-to-close log-returns for the S&P 500 index and the panel of SPX option prices. We use the realized kernel estimator, by Barndorff-Nielsen et al. (2008), as our realized measure of volatility, where the realized kernel is implemented with the Parzen kernel.[8]

Our sample spans the period from January 1990 to December 2019, which has 7,559 trading days. The option prices are assembled from two different databases. Option price data for the first six years are based on the Optsum data from the CBOE DataShop, whereas option prices, 1996 or later, are based on the OptionMetrics data. We use out-of-the-money put and call options with positive trading volume and with maturity between two weeks and six months and we apply the filters proposed by Bakshi et al. (1997). We only use Wednesday option prices, as is common in this literature. For each maturity, we retain the three strike prices with the highest liquidity (as defined by daily trading volume).[9] This results in a total of 32,024 option prices.

Table 1 reports descriptive statistics for S&P 500 returns, realized kernels, and CBOE VIX in Panel A. The S&P 500 returns exhibit a small negative skewness and a high level of kurtosis. The realized kernel and the VIX are both positively skewed and leptokurtic. The standard deviation of returns is, at 17.437%, substantially smaller than the average option-implied volatility, at 19.147%. Their difference reflects the (average) negative variance risk premium. Panel B of Table 1 provides an extensive summary of the number of contracts, average prices, and the average implied volatility within each subcategory in our option data set. Following Christoffersen et al. (2014), the out-of-the-money put options are converted to in-the-money call options using put-call parity, and the Black-Scholes delta is used to measure the moneyness of options. The option prices included in our analysis are all out-of-the-money options. So, options with deltas larger than 0.5 are out-of-the-money put options, and options with deltas less than 0.5 are out-of-the-money call options. In the upper part of panel B, it can be seen that deep out-of-the-money put options (deltas above 0.7) are relatively expensive compared with out-of-the-money calls, which reflects the well-known volatility smirk when implied volatility is plotted against moneyness. The middle part of the panel B summarizes features of the option prices when sorted by maturity, and the implied volatility term

[8]The S&P 500 index was collected from Yahoo Finance. The realized measure was obtained from the Realized Library of Oxford-Man institute for the years 2000–2019. Before 2000 we used high-frequency data on S&P 500 futures prices (front-month continuous) from TickData to construct the realized kernels.

[9]The same type of inclusion criteria were used in Christoffersen et al. (2014) and Huang et al. (2017), who retained the six most liquid strike prices with maturities between two weeks and six months.

structure is roughly flat on average. The bottom of Panel B sorts the data by the volatility state as measured by contemporary VIX level and, as expected, the implied volatility increases in VIX.

6.2 Parameter Estimation

We present results for the Markov-switching Realized GARCH model with two states ($N = 2$).[10] In Table 2, we present the estimation results for each of the models. Parameters are estimated using the sample from January 1990 to December 2019. The estimated parameters are given along with their robust standard errors in brackets. We also report implied logarithmically transformed expectation of h_t, and the implied persistence of volatility dynamics, $\pi^{\mathbb{P}}$ and $\pi^{\mathbb{Q}}$, under the physical and risk-neutral measures, respectively. The values of the maximized log-likelihood, ℓ_{Total}, are provided. The maximized log-likelihoods are not comparable unless the underlying models describe the same data, which is not the case for all models. The first four models are GARCH-type models, which largely share a common notation for their parameters. To conserve space, we present the estimates for σ (for MS-RG and RG) and ρ (for GARV) on the same line. The last model is the LHARG model, which has a different set of parameters and these are labelled in a separate column.[11]

The estimated models are consistent with several stylized facts in the related literature. First, the estimated models imply a highly persistent volatility process under both physical and risk-neutral measures. The only exception is the LHARG model which estimates the volatility to be less persistent, in particular under the physical measure. The likely explanation is that the LHARG model treats the noisy realized measure as the true underlying volatility. It is well known that the measurement errors in the realized measure will induce a downwards bias in autocorrelations, see Hansen and Lunde (2014), and this may explain the lower estimate of persistence in this model. Second, all of the models estimate the equity premium parameter to be positive, $\lambda > 0$, and significant. Third, the values of the variance risk parameter (χ) all indicate a significant negative variance risk premium[12] and higher risk-neutral volatility than their physical counterparts. Fourth, the models find the leverage effect, as indicated by τ_1 (and γ for LHARG), to be significant. Fifth, the two Realized GARCH models (columns 1 and 2), estimate the parameter, γ, to be positive and significant. This parameter measures the contribution of the realized volatility measure in describing the

[10] The number of states could be chosen by a suitable statistical criterion. Nevertheless, a model with two states will likely be preferred in many applications because additional states add many parameters to the model, and a two-state model already adds a high degree of flexibility to the model structure.

[11] The logarithm of unconditional variances are estimated instead of the intercepts in the variance equations, which are then implied from the unconditional variance formulas.

[12] Positive χ for MS-RG, RG, GARV models, and χ greater than one for HNG, LHARG models corresponds to a negative variance risk premium.

Table 1: Summary Statistics

A: S&P 500 returns, Realized Kernels and CBOE VIX

	Mean(%)	Std(%)	Skewness	Kurtosis	Obs.
Returns (annualized)	7.377	17.437	-0.267	11.851	7,559
Realized Kernels (annualized)	12.050	8.335	3.415	23.948	7,559
CBOE VIX	19.147	7.725	2.132	10.955	7,559

B: SPX Option Price Data

	Implied Volatility (%)	Average price ($)	Obs.
All options	17.53	84.24	32,024
Partitioned by moneyness			
Delta$<$0.3	13.05	10.73	4,475
0.3$\leq$Delta$<$0.4	13.93	19.38	2,464
0.4$\leq$Delta$<$0.5	15.07	30.81	3,093
0.5$\leq$Delta$<$0.6	17.09	46.38	4,449
0.6$\leq$Delta$<$0.7	18.16	64.92	4,178
0.7$\leq$Delta	20.22	151.81	13,365
Partitioned by maturity			
DTM$<$30	15.48	45.80	8,255
30$\leq$DTM$<$60	17.15	75.67	8,506
60$\leq$DTM$<$90	18.74	90.21	5,771
90$\leq$DTM$<$120	19.19	113.89	4,338
120$\leq$DTM$<$150	18.74	125.86	2,642
150$\leq$DTM	18.65	130.84	2,512
Partitioned by the level of VIX			
VIX$<$15	13.04	80.51	14,746
15$\leq$VIX$<$20	17.59	88.61	8,792
20$\leq$VIX$<$25	21.91	86.30	4,851
25$\leq$VIX$<$30	25.74	88.97	1,965
30$\leq$VIX$<$35	29.85	86.80	856
35$\leq$VIX	39.37	78.06	814

Note: Summary statistics for close-to-close S&P 500 index returns, realized kernels (in square root), CBOE VIX, and SPX option prices from January 1990 to December 2019. The reported statistics for S&P 500, realized kernels, and VIX index include the sample mean (Mean), standard deviation (Std), skewness (Skew), kurtosis (Kurt), and the number of observations (Obs). Option prices are based on closing prices of out-of-the-money call and put options. Out-of-the-money put options are converted to in-the-money call options using put-call parity. We report the average Black-Scholes implied volatility (IV), average price, and the number of option prices for different partitions of option prices. "Moneyness" is defined by the Black-Scholes delta. DTM denotes the number of calendar days to maturity. Data sources: S&P 500 returns from Yahoo Finance; VIX from CBOE's website; Realized kernels from TickData (1990-1999) and Realized Library of Oxford-Man institute (2000-2019); Option prices from Optsum data (1990–1995) and OptionMetrics (1996–2019).

Table 2: Estimation Results

Model	MS-RG	RG	GARV	HNG		LHARG
λ	0.0354	0.0359	0.2254	2.9196	λ	2.8969
	(0.0103)	*(0.0092)*	*(0.0247)*	*(0.7198)*		*(0.3353)*
β	0.8435	0.8741	0.9776	0.6601	θ	4.14E-05
	(0.0002)	*(0.0002)*	*(0.0033)*	*(0.0231)*		*(3.97E-06)*
τ_1	-0.1520	-0.1157	249.89	468.59	δ	1.2182
	(0.0007)	*(0.0011)*	*(22.88)*	*(31.17)*		*(0.0846)*
τ_2	-0.0080	0.0030	3.16E-07	1.49E-06	β_d	0.2060
	(0.0009)	*(0.0017)*	*(1.63E-08)*	*(7.55E-08)*		*(0.0247)*
γ	0.1278	0.1083	0.3056		β_w	0.2456
	(0.0016)	*(0.0035)*	*(0.0156)*			*(0.0192)*
ϕ	0.9930	0.9952	9.23E-08		β_m	0.2944
	(0.0035)	*(0.0014)*	*(1.67E-03)*			*(0.0178)*
δ_1	-0.1733	-0.1641	629.75		α_d	4.70E-06
	(0.0091)	*(0.0091)*	*(0.72)*			*(2.59E-07)*
δ_2	0.1548	0.1707	2.47E-06		α_w	8.22E-06
	(0.0094)	*(0.0129)*	*(9.59E-11)*			*(3.55E-07)*
σ, ρ	0.6306	0.6249	0.3961		α_m	1.74E-10
	(0.0066)	*(0.0065)*	*(0.0153)*			*(2.59E-07)*
ξ		-0.8212	0.0584		γ	409.56
		(0.0111)	*(0.0036)*			*(21.53)*
ξ_{Low}	-0.8767					
	(0.0454)					
ξ_{High}	-0.7788					
	(0.0349)					
χ		0.0519	6.5567	1.1512	χ	1.0947
		(0.0129)	*(0.6418)*	*(0.0222)*		*(0.0101)*
χ_{Low}	-0.0052					
	(0.0022)					
χ_{High}	0.4586					
	(0.0109)					
$\pi_{\text{Low\|Low}}$	0.9996					
	(0.0072)					
$\pi_{\text{High\|High}}$	0.9948					
	(0.0025)					
$\sigma_e \times 100$	2.4155	2.8190	2.9756	3.4506	$\sigma_e \times 100$	3.1869
$\log \mathbb{E}(h_t)$	-9.3672	-9.0763	-9.0241	-9.0665	$\log \mathbb{E}(h_t)$	-9.4541
$\pi^{\mathbb{P}}$	0.9704	0.9818	0.9974	0.9871	$\pi^{\mathbb{P}}$	0.7460
$\pi^{\mathbb{Q}}$	0.9704	0.9818	0.9974	0.9912	$\pi^{\mathbb{Q}}$	0.8503
$\ell^{\mathbb{P}}$	17980	17964	84469	24848	$\ell^{\mathbb{P}}$	89553
$\ell^{\mathbb{Q}}$	17418	16251	15833	14723	$\ell^{\mathbb{Q}}$	15329
ℓ_{Total}	35398	34215	100302	39571	ℓ_{Total}	104882

Note: Estimation results for the full sample period (January 1990 to December 2019). The first row refers to model specification. Parameter estimates are reported with robust standard errors (in parentheses), $\pi^{\mathbb{P}}$ and $\pi^{\mathbb{Q}}$ refer to the volatility persistence under $\mathbb{P}$ and $\mathbb{Q}$, respectively. The value of the log-likelihood function is reported at the bottom of the table where $\ell^{\mathbb{P}} = \ell_{R,x}$ are the terms of the log-likelihood related to returns and realized measures and $\ell^{\mathbb{Q}} = \ell_o$ is the part of the log-likelihood related to option prices.

volatility dynamics, and the realized measures are found to be an important predictor. The estimate of ϕ is close to one, which implies that the realized measure is proportional to the conditional variance. This reinforces the label *measurement equation* for (3) and (3'). Compared with other models in Table 2, the two Realized GARCH models deliver the smallest Vega-weighted pricing error σ_e.

The estimation results for the Markov-switching Realized GARCH model (MS-RG), proposed in this paper, are quite interesting. First, the state-dependent intercept ξ does improve the empirical fit of the model, as illustrated by the increased value of the log-likelihood for the "physical" variables $\ell^{\mathbb{P}}$. The parameter ξ controls the long-run volatility level within each state. For this reason, we adopt labels "Low" and "High" to denote the low- and high-volatility states, respectively. Second, we also find the estimated variance risk premium parameter, χ, to be state-dependent. In the high-volatility state, χ_{High} is estimated to be 0.4586, and is highly significant. This estimate translates to a large negative variance risk premium (in absolute value). In the low-volatility state, we estimate χ_{Low} to be a small negative value, which suggests that investors have a slight appetite for variance risk in this state, *i.e.* a positive variance risk premium. The difference between these two estimates reinforces the value of introducing a state-dependent pricing kernel. The estimate of χ in single-state RG model is 0.0519, which falls between χ_{High} and χ_{Low}. Third, the estimated transition probabilities within the same state ($\pi_{\text{High|High}}$ and $\pi_{\text{Low|Low}}$) are both near one, which implies the time-varying process of the hidden states is highly persistent. Fourth, although we focus on the model with two states, the improvements relative to the benchmark model are impressive. The MS-RG model lowers the Vega-weighted pricing error σ_e by 14.3% relative to the single-state RG model.

In Figure 2, we present the time series of conditional state probabilities along with the VIX index. The blue solid line denotes the estimated value of $P_t(s_t = \text{"High"})$, and the red dashed line is the logarithmically transformed VIX index. The "High" volatility state is also the state with the highest variance risk premium (in absolute value), so a large value of $P_t(s_t = \text{"High"})$ is a period where investors have relatively high variance risk aversion. There is a great deal of variation in $P_t(s_t = \text{"High"})$ over time and the process is very persistent because π_{ii} is estimated to be close to one. There are several period, where $P_t(s_t = \text{"Low"}) = 1 - P_t(s_t = \text{"High"}) \simeq 1$, including most of the time during the year, 1993-1995, 2004-2007, and 2014-2017. These are times where investors have an appetite for variance risk (or very low volatility risk aversion). Investors demand additional compensation for taking on variance risk in the "High" volatility state. The onset of these periods often coincides with large jumps in the VIX index, such as those seen around the time of the Asian Crisis in 1997, the bursting of the dot-com bubble and corporate scandals in early

2000s, the global financial crises, and the Euro crisis. A large component of the VIX is, according to Bekaert et al. (2013), driven by factors that relate to time-varying risk-aversion. The commonality between $P_t(s_t = \text{“High”})$ and the VIX supports this view, and the clear pattern that large upwards jumps in these two series tend to coincide.

6.3 Option Pricing Performance

In this section, we turn to the models' ability to price options, first in-sample and then out-of-sample. We follow the existing literature and convert option prices to their corresponding implied volatilities, as defined by the Black–Scholes formula. We evaluated each of the models by comparing observed implied volatility, denoted by $\text{IV}^{\text{Market}}$, to the corresponding model-based implied volatility, denoted IV^{Model}. The criterion used in our evaluation is the root mean squared error (RMSE),

$$\text{RMSE}_{\text{IV}} = \sqrt{\frac{1}{N}\sum_{i=1}^{N}\left(\text{IV}_i^{\text{Model}} - \text{IV}_i^{\text{Market}}\right)^2} \times 100,$$

where $i = 1,\ldots,N$ indexes each of the option prices (converted to implied volatilities) that were included in the sample period.

6.3.1 In-sample Option Pricing

In Table 3 we report the in-sample performance for option pricing for each of the estimated models. The RMSEs are reported in the first row and we find the MR-RG to have the smallest RMSE followed by the RG. The HNG has the largest average RMSE. The percentage reduction in RMSE of the MS-RG model relative to each of the alternative models ranges from 15.3% to 30.8%.

In order to investigate if the improvements by the MS-RG model are seen for options with specific characteristics or are found across the board, we repeat the comparisons after sorting the options by moneyness, time to maturity, and the contemporaneous level of the VIX.

Sorting by moneyness can cast light on the models' ability to generate sufficient leverage effect. The MS-RG model has the smallest RMSE in all subcategories. Relative to the single-state RG model, the two-state MS-RG model performs particularly well at pricing deep out-of-the-money call options (Delta$<$0.3), with the reduction in RMSE up to 21%.

Maturity is related to the models' ability to explain volatility dynamics over longer time spans. The RMSEs of the MS-RG model are fairly uniform along this dimension and the MS-RG model also has the smallest RMSE across all subcategories. The RMSE of the MS-RG is a tad higher at

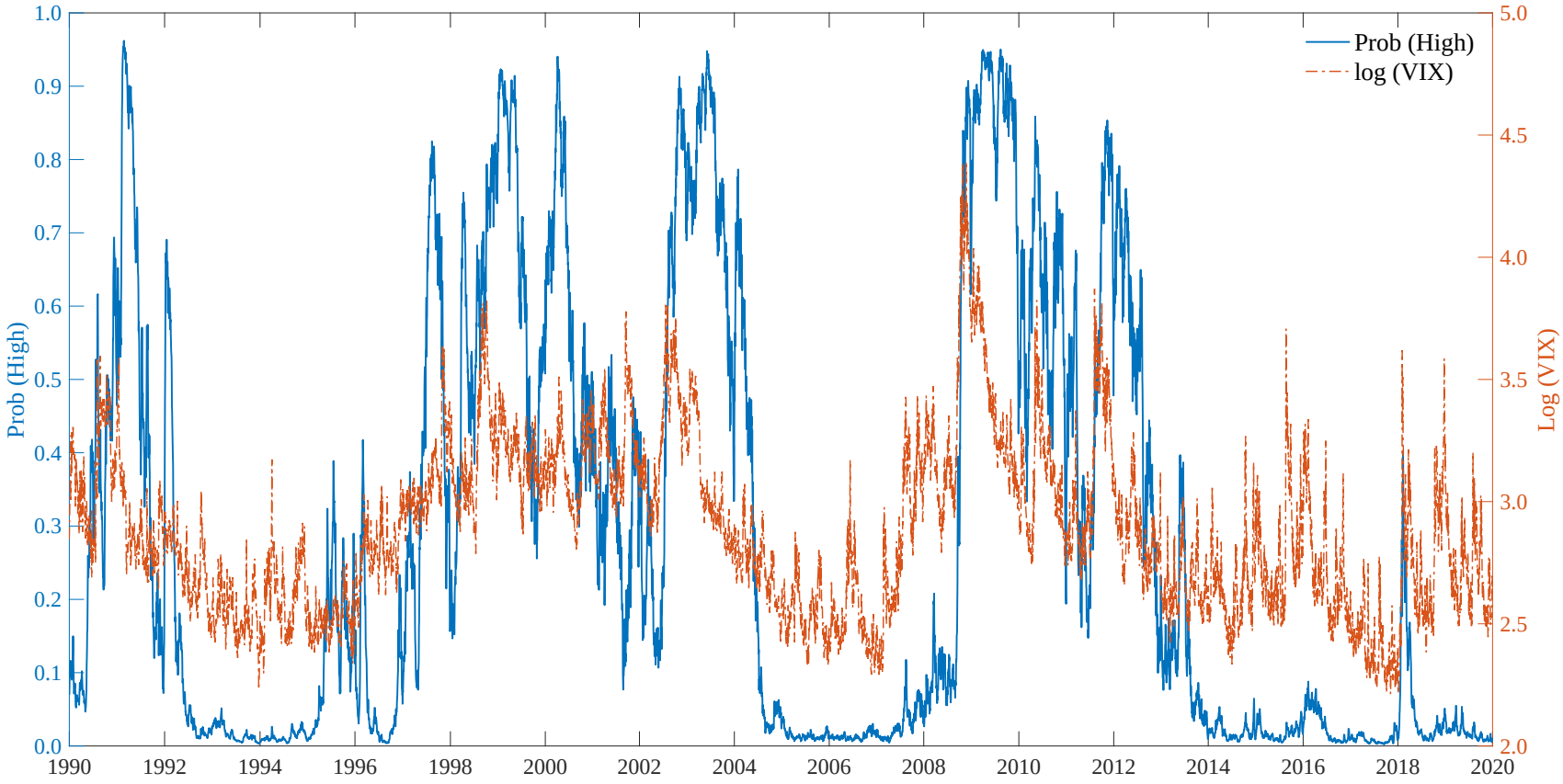


Figure 2: This figure presents the time series of conditional probabilities in "High"-volatility state $\text{Prob}_t(\text{High})$ (blue solid line), and log (VIX) (red dashed line). The correlation between these two series is 56.89%.

Table 3: Option Pricing Performance (In-sample)

Model	MS-RG	RG	GARV	LHARG	HNG
Total $RMSE_{IV}$	2.4190	2.8564	2.9597	3.1633	3.4955
Partitioned by moneyness					
Delta<0.3	2.4054	3.0533	2.9437	3.0871	3.5852
0.3≤Delta<0.4	2.3072	2.7440	2.6584	3.2202	3.4494
0.4≤Delta<0.5	2.2396	2.5964	2.4270	2.9568	3.2505
0.5≤Delta<0.6	2.5395	2.9568	2.7650	3.3448	3.4288
0.6≤Delta<0.7	2.6245	2.9730	2.9863	3.3649	3.5866
0.7≤Delta	2.3738	2.7942	3.1830	3.0934	3.5230
Partitioned by maturity					
DTM<30	2.4658	2.7672	2.8327	2.7448	3.6105
30≤DTM<60	2.3509	2.8310	2.9129	3.0095	3.4881
60≤DTM<90	2.3949	2.9086	3.1281	3.4383	3.5600
90≤DTM<120	2.3609	2.8741	2.8234	3.3095	3.3103
120≤DTM<150	2.3939	2.8091	3.1161	3.4983	3.3422
150≤DTM	2.6617	3.1234	3.1910	3.6585	3.4487
Partitioned by the level of VIX					
VIX<15	1.5403	1.8446	1.6880	1.8466	2.3889
15≤VIX<20	2.4148	2.5489	2.4099	2.4991	3.2568
20≤VIX<25	2.9759	3.6254	3.9540	4.1993	4.4586
25≤VIX<30	3.0672	4.0626	4.8481	5.0164	4.7876
30≤VIX<35	3.4921	4.8279	6.1206	5.9721	5.4262
35≤VIX	6.0232	6.8771	6.5122	7.9058	7.6930

Note: This table reports the in-sample option pricing performance for each model in Table 2 (January 1990 to December 2019). We evaluate the model's option pricing ability through the root of mean square errors of implied volatility ($RMSE_{IV}$). We summarize the results by option moneyness, maturity and market VIX level. Moneyness is measured by Delta computed from the Black-Scholes model. DTM denotes the number of calendar days to maturity.

the longest maturity compared to shorter maturities, but its RMSE is still substantially smaller than that of all competitors.

Finally, the comparisons across levels of the volatility index will illustrate the models' ability to generate a proper variance risk premium at different levels of volatility. Along this dimension, we also find that the MS-RG model has the smallest RMSE in all subcategories. The RMSEs are roughly proportional to the level of VIX, which is what one would expect if the distribution of pricing errors, when measured in percentage, is relatively homogeneous across subcategories.

Table 4: Option Pricing Performance (Out-of-sample)

Model	MS-RG	RG	GARV	LHARG	HNG
Total $RMSE_{IV}$	2.4835	2.9903	3.2957	3.2960	3.7891
Partitioned by moneyness					
Delta<0.3	2.5241	3.6791	4.0796	4.1773	5.0360
0.3≤Delta<0.4	2.3688	3.1397	3.8544	3.9975	4.4769
0.4≤Delta<0.5	2.1955	2.7655	3.4133	3.4129	3.9895
0.5≤Delta<0.6	2.5905	2.8695	3.5277	3.6684	3.8401
0.6≤Delta<0.7	2.5965	2.7067	3.3051	3.3755	3.6698
0.7≤Delta	2.4840	2.8429	2.7337	2.5642	3.0452
Partitioned by maturity					
DTM<30	2.4336	2.9509	2.6322	2.4480	3.9714
30≤DTM<60	2.3502	3.1034	2.9061	2.9161	3.7961
60≤DTM<90	2.4637	3.0227	3.3932	3.5187	3.5975
90≤DTM<120	2.6948	2.9482	3.7651	3.8349	3.6696
120≤DTM<150	2.4959	2.8202	4.2091	4.2501	3.6615
150≤DTM	2.7251	2.9157	4.3636	4.3744	3.8217
Partitioned by the level of VIX					
VIX<15	1.6727	2.0883	2.5067	2.4860	3.4768
15≤VIX<20	2.5730	3.1371	3.1802	2.7744	3.5961
20≤VIX<25	3.2861	3.9875	3.8534	3.5819	3.6284
25≤VIX<30	3.3513	4.3955	4.8263	4.7979	3.8781
30≤VIX<35	3.2173	4.6628	5.3971	5.9139	4.7166
35≤VIX	5.5187	5.9686	7.7183	9.6217	8.5992

Note: This table reports the out-of-sample option pricing performance. We evaluate the model's option pricing ability through the root of mean square errors of implied volatility ($RMSE_{IV}$). We summarize the results by option moneyness, maturity and market VIX level. Moneyness is measured by Delta computed from the Black-Scholes model. DTM denotes the number of calendar days to maturity. We conduct our out-of-sample performance evaluation by equally splitting our original dataset into two subsamples: the in-sample data consists of the first 15 years (1990-2004) and the out-of-sample consists of the remaining 15 years (2005-2019). The estimation for each model is done only once for the in-sample data, and then price the out-of-sample data by the estimated parameters.

6.3.2 Out-of-sample Option Pricing

In this section, we turn to out-of-sample comparisons of the pricing models. A Markov switching model is more heavily parameterized and this can lead to overfitting when the model is estimated and evaluated with the same data. Here we follow Christoffersen and Jacobs (2004) and split the original sample into two subsamples. We use the first 15 years, 1990-2004, exclusively for model estimation (in-sample) and use the remaining 15 years, 2005-2019, for model evaluation (out-of-sample) of the estimated models. So, each of the models is estimated exactly once using the in-sample data and their abilities to price options are exclusively evaluated over the out-of-sample period.

We report the out-of-sample RMSEs in Table 4. The relative ranking of the models is identical to the relative ranking we found in-sample. The MS-RG model continues to be the best-performing model. Not only is the MS-RG model the best on average, but it is also the best within all subcategories. Impressively, the MS-RG has nearly the same RMSE out-of-sample as it does in-sample. Given the great out-of-sample performance by the MS-RG, we conclude that its better option pricing performance is not a result of overfitting, but rather reflects a real and substantive improvement in model-based option pricing, which can be attributed to the time-varying risk aversion that the MS-RG model can capture.

7 Conclusion

We introduced Markov-switching to the Realized GARCH model and combined it with an exponentially affine pricing kernel with a time-varying aversion to volatility risk. A key feature of this framework is that time-variation in the pricing kernel is introduced with the same hidden Markov process that is used in the Realized GARCH model. In this way, the hidden Markov chain process brings time-variation in both the physical measure and the risk-neutral measure. We derived model-implied pricing formula for European options in this framework. This was achieved with an analytical approximation method that is based on an Edgeworth expansion of the density for cumulative return.

The MS-RG model is straightforward to estimate from returns and realized volatilities by quasi maximum likelihood estimation. Volatility models with a hidden Markov-switching are typically challenging to estimate. We circumvent the usual complications by introducing Markov switching in a manner where states probabilities can be inferred from the realized measures and returns. Estimating the parameters in the pricing kernel is more involved and requires that option prices are

included in the empirical analysis. We estimated the model with a large panel of option prices using 30 years of data (from 1990 to 2019) and find that investors have a state-dependent tolerance for volatility-specific risk. Consistent with the existing literature, we find that the volatility risk premium is, on average, negative. However, there are periods when investors appear to have an appetite for variance risk. These periods tend to coincide with relatively low levels of the VIX. During other periods, we find that investors have a relatively high aversion to volatility risk, and these periods are often preceded by sudden upwards jumps in the VIX.

We compared the proposed model with several benchmarks and found it to outperform all competing models. The option pricing model that is based on the MS-RG framework leads to substantial improvements in option pricing. This reduction in the RMSE of option pricing errors range from 15.3% to 30.8% relative to the alternative models. The same magnitudes of improvements are seen across options with different characteristics. These improvements are also seen out-of-sample, where the RMSE reductions in option pricing errors range from 17% to 34.5%.

8 Data Availability Statement

The S&P 500 index was collected from Yahoo Finance and CBOE VIX is from the CBOE website. The SPX options are available from the Optsum data (1990–1995) and OptionMetrics (1996–2019). The realized measure of volatility was obtained from the Realized Library of Oxford-Man institute (2000-2019) and TickData (1990-1999).

References

Aingworth, D. D., Das, S. R., and Motwani, R. (2006). A simple approach for pricing equity options with Markov switching state variables. *Quantitative Finance*, 6(2):95–105.

Aït-Sahalia, Y. and Lo, A. W. (2000). Nonparametric risk management and implied risk aversion. *Journal of Econometrics*, 94(1–2):9–51.

Bakshi, G., Cao, C., and Chen, Z. (1997). Empirical performance of alternative option pricing models. *The Journal of Finance*, 52(5):2003–2049.

Bakshi, G., Madan, D., and Panayotov, G. (2010). Returns of claims on the upside and the viability of U-shaped pricing kernels. *Journal of Financial Economics*, 97(1):130–154.

Barndorff-Nielsen, O. E., Hansen, P. R., Lunde, A., and Shephard, N. (2008). Designing realised kernels to measure the ex-post variation of equity prices in the presence of noise. *Econometrica*, 76(6):1481–536.

Bekaert, G., Engstrom, E. C., and Xu, N. R. (2021). The time variation in risk appetite and uncertainty. *Management Science*. Forthcoming.

Bekaert, G., Hoerova, M., and Duca, M. L. (2013). Risk, uncertainty and monetary policy. *Journal of Monetary Economics*, 60(7):771–788.

Cai, J. (1994). A Markov model of switching-regime arch. *Journal of Business & Economic Statistics*, 12(3):309–316.

Campbell, J. Y. and Cochrane, J. H. (1999). By force of habit: A consumption-based explanation of aggregate stock market behavior. *Journal of Political Economy*, 107(2):205–251.

Chabi-Yo, F., Garcia, R., and Renault, E. (2008). State dependence can explain the risk aversion puzzle. *Review of Financial Studies*, 21(2):973–1011.

Chen, C.-C. and Hung, M.-Y. (2010). Option pricing under Markov-switching GARCH processes. *Journal of Futures Markets: Futures, Options, and Other Derivative Products*, 30(5):444–464.

Christoffersen, P., Feunou, B., Jacobs, K., and Meddahi, N. (2014). The economic value of realized volatility: Using high-frequency returns for option valuation. *Journal of Financial and Quantitative Analysis*, 49(3):663–697.

Christoffersen, P., Heston, S. L., and Jacobs, K. (2013). Capturing option anomalies with a variance-dependent pricing kernel. *Review of Financial Studies*, 26(8):1963–2006.

Christoffersen, P. and Jacobs, K. (2004). Which GARCH model for option valuation? *Management Science*, 50(9):1204–1221.

Christoffersen, P., Jacobs, K., and Ornthanalai, C. (2012). Dynamic jump intensities and risk premiums: Evidence from S&P500 returns and options. *Journal of Financial Economics*, 106(3):447–472.

Corsi, F., Fusari, N., and Vecchia, D. L. (2013). Realizing smiles: Options pricing with realized volatility. *Journal of Financial Economics*, 107(2):284–304.

Creal, D., Koopman, S. J., and Lucas, A. (2013). Generalized Autoregressive Score Models With Applications. *Journal of Applied Econometrics*, 28(5):777–795.

Daouk, H. and Guo, J. Q. (2004). Switching asymmetric GARCH and options on a volatility index. *Journal of Futures Markets: Futures, Options, and Other Derivative Products*, 24(3):251–282.

Duan, J.-C., Gauthier, G., and Simonato, J. (1999). An analytical approximation for the GARCH option pricing model. *Journal of Computational Finance*, 2(4):75–116.

Duan, J.-C., Popova, I., and Ritchken, P. (2002). Option pricing under regime switching. *Quantitative Finance*, 2(2):116–132.

Elliott, R. J., Siu, T. K., and Chan, L. (2006). Option pricing for GARCH models with Markov switching. *International Journal of Theoretical and Applied Finance*, 9(6):825–841.

Gray, S. F. (1996). Modeling the conditional distribution of interest rates as a regime-switching process. *Journal of Financial Economics*, 42(1):27–62.

Grith, M., Härdle, W. K., and Krätschmer, V. (2017). Reference-dependent preferences and the empirical pricing kernel puzzle. *Review of Finance*, 21(1):269–298.

Hamilton, J. D. and Susmel, R. (1994). Autoregressive conditional heteroskedasticity and changes in regime. *Journal of Econometrics*, 64(1-2):307–333.

Hansen, P. R. and Huang, Z. (2016). Exponential GARCH modeling with realized measures of volatility. *Journal of Business & Economic Statistics*, 34(2):269–287.

Hansen, P. R., Huang, Z., and Shek, H. (2012). Realized GARCH: A joint model of returns and realized measures of volatility. *Journal of Applied Econometrics*, 27(6):877–906.

Hansen, P. R. and Lunde, A. (2014). Estimating the persistence and the autocorrelation function of a time series that is measured with error. *Econometric Theory*, 30(1):60–93.

Hansen, P. R. and Tong, C. (2021). Option pricing with time-varying volatility risk aversion. *arXiv:submit/4262330*.

Heston, S. L. and Nandi, S. (2000). A closed-form GARCH option valuation model. *Review of Financial Studies*, 13:585–625.

Huang, Z., Tong, C., and Wang, T. (2019). VIX term structure and VIX futures pricing with realized volatility. *Journal of Futures Markets*, 39(1):72–93.

Huang, Z., Wang, T., and Hansen, P. R. (2017). Option pricing with the realized GARCH model: An analytical approximation approach. *Journal of Futures Markets*, 37:328–358.

Jackwerth, J. C. (2000). Recovering risk aversion from option prices and realized returns. *The Review of Financial Studies*, 13:433–451.

Jarrow, R. and Rudd, A. (1982). Approximate option valuation for arbitrary stochastic processes. *Journal of Financial Economics*, 10(3):347 – 369.

Kiesel, R. and Rahe, F. (2017). Option pricing under time-varying risk-aversion with applications to risk forecasting. *Journal of Banking & Finance*, 76:120–138.

Klaassen, F. (2002). Improving GARCH volatility forecasts with regime-switching GARCH. *Empirical Economics*, 27(2):363–394.

Li, G. (2007). Time-varying risk aversion and asset prices. *Journal of Banking & Finance*, 31:243–257.

Liew, C. C. and Siu, T. K. (2010). A hidden Markov regime-switching model for option valuation. *Insurance: Mathematics and Economics*, 47(3):374–384.

Lucas, R. E. (1978). Asset prices in an exchange economy. *Econometrica*, 46:1429–1445.

Majewski, A. A., Bormetti, G., and Corsi, F. (2015). Smile from the past: A general option pricing framework with multiple volatility and leverage components. *Journal of Econometrics*, 187:521–531.

Ornthanalai, C. (2014). Levy jump risk: Evidence from options and returns. *Journal of Financial Economics*, 112(1):69–90.

Polkovnichenko, V. and Zhao, F. (2013). Probability weighting functions implied in options prices. *Journal of Financial Economics*, 107:580–609.

Rosenberg, J. V. and Engle, R. F. (2002). Empirical pricing kernels. *Journal of Financial Economics*, 64:341–372.

Satoyoshi, K. and Mitsui, H. (2011). Empirical study of Nikkei 225 options with the Markov switching GARCH model. *Asia-Pacific Financial Markets*, 18(1):55–68.

Shen, Y., Fan, K., and Siu, T. K. (2014). Option valuation under a double regime-switching model. *Journal of Futures Markets*, 34(5):451–478.

Tong, C. and Huang, Z. (2021). Pricing VIX options with realized volatility. *Journal of Futures Markets*, 41(8):1180–1200.

[dataset] Yahoo Finance (2021). S&P 500 Index. https://finance.yahoo.com/quote/%5EGSPC/history.

[dataset] CBOE VIX (2021). https://www.cboe.com/tradable_products/vix/vix_historical_data/.

[dataset] The Oxford-Man Realized Library (2021). The Realized Kernels of S&P 500 Index. https://realized.oxford-man.ox.ac.uk/data/download.

[dataset] TickData (2021). High-frequency S&P 500 Futures Prices. https://www.tickdata.com.

[dataset] OptionMetrics (2021). SPX Options. https://optionmetrics.com.

[dataset] CBOE DataShop (2021). SPX Options. https://datashop.cboe.com/option-quotes.

A Appendix of Proofs

Proof that $\psi = -\lambda$

Imposing the no-arbitrage condition $\mathbb{E}_t^{\mathbb{Q}}[\exp(R_{t+1})] = \exp(r)$ yields

$$\begin{aligned} \mathbb{E}_t^{\mathbb{Q}}[\exp(R_{t+1})] &= \mathbb{E}_t^{\mathbb{P}}[\mathbb{E}_t^{\mathbb{P}}[M_{t+1,t}(s_{t+1})\exp(R_{t+1})|s_{t+1}]] \\ &= \exp\left[r + (\lambda+\psi)\mathbb{E}_t^{\mathbb{P}}\sqrt{h_{t+1}}\right] = \exp(r), \end{aligned} \tag{A.1}$$

which shows that $\psi = -\lambda$.

□

Proof of Theorem 1. The MGF of $z_{t+1}^* \equiv z_{t+1} - \psi$ and $u_{t+1}^* = u_{t+1} - \chi_{s_{t+1}}$ under $\mathbb{Q}$ is

$$\begin{aligned} & \mathbb{E}_t^{\mathbb{Q}}\left[\exp(\theta_1 z_{t+1}^* + \theta_2 u_{t+1}^*)\right] \\ = \; & \mathbb{E}_t^{\mathbb{P}}\left[M_{t+1,t}(s_{t+1})\exp(\theta_1 z_{t+1}^* + \theta_2 u_{t+1}^*)\right] \\ = \; & \mathbb{E}_t^{\mathbb{P}}\left\{\mathbb{E}_t^{\mathbb{P}}\left[M_{t+1,t}(s_{t+1})\exp(\theta_1 z_{t+1}^* + \theta_2 u_{t+1}^*)|s_{t+1}\right]\right\} \\ = \; & \mathbb{E}_t^{\mathbb{P}}\left\{\mathbb{E}_t^{\mathbb{P}}\left[M_{t+1,t}(s_{t+1})\exp(\theta_1 z_{t+1} - \theta_1\psi + \theta_2 u_{t+1} - \theta_2\chi_{s_{t+1}})|s_{t+1}\right]\right\} \\ = \; & \mathbb{E}_t^{\mathbb{P}}\left\{\exp\left(\frac{1}{2}(\theta_1+\psi)^2 + \frac{1}{2}\left(\theta_2 + \chi_{s_{t+1}}\right)^2 - \theta_1\psi - \theta_2\chi_{s_{t+1}} - \frac{1}{2}\psi^2 - \frac{1}{2}\chi_{s_{t+1}}^2\right)\right\} \\ = \; & \exp\left(\frac{1}{2}\theta_1^2 + \frac{1}{2}\theta_2^2\right) \end{aligned}$$

which shows $z_{t+1}^* \equiv z_{t+1} - \psi$ and $u_{t+1}^* = u_{t+1} - \chi_{s_{t+1}}$ are i.i.d. $N(0,1)$ in $\mathbb{Q}$.

□

Proof of Corollary 1. Note that the dynamic of $\log h_t$ in $\mathbb{Q}$-measure can be written as

$$\begin{aligned} \log h_{t+1} &= \underbrace{\omega^* + \gamma\xi_{s_t}^*}_{\zeta' s_t} + \underbrace{(\beta+\gamma\phi)}_{\rho}\log h_t + \underbrace{(\tau_1^* + \gamma\delta_1^*)z_t^* + (\tau_2+\gamma\delta_2)(z_t^{*2}-1) + \gamma\sigma u_t^*}_{v_t} \\ &= \zeta' s_t + \rho\log h_t + v_t \end{aligned}$$

where $\zeta \in \mathbb{R}^{N\times 1}$, with $\zeta_j = \omega^* + \gamma\xi_j^*,\ j = 1,\ldots,N$. The logarithm of the MGF of v_t, denoted as $G(\theta) = \log\mathbb{E}_t^{\mathbb{Q}}[\exp(\theta v_{t+1})]$, is given by

$$G(\theta) = -\frac{1}{2}\log(1-2\theta(\tau_2+\gamma\delta_2)) - \theta(\tau_2+\gamma\delta_2) + \frac{\theta^2(\tau_1^*+\gamma\delta_1^*)^2}{2-4\theta(\tau_2+\gamma\delta_2)} + \frac{1}{2}\gamma^2\sigma^2\theta^2.$$

Note that the MGF of s_t, for any vector $\varphi \in \mathbb{R}^{N\times 1}$, is given by

$$\begin{aligned}\mathbb{E}_t^{\mathbb{Q}}\left[\exp(\varphi' s_{t+1})\middle| s_t\right] &= \mathbb{E}_t^{\mathbb{P}}\left[\exp(\varphi' s_{t+1})\middle| s_t\right] = \mathbb{E}_t^{\mathbb{P}}\left[\exp\left(\sum_{i=1}^{N}\varphi_i s_{t+1,i}\right)\middle| s_t\right] \\ &= \sum_{i=1}^{N}\left(\sum_{j=1}^{N}\pi_{ij}\exp(\varphi_j)\right)s_{t,i} = \exp\left(\Delta'(\varphi)s_t\right)\end{aligned} \tag{A.2}$$

where the vector function $\Delta(\varphi)$ is defined by

$$\Delta_i(\varphi) \equiv \log\left(\sum_{j=1}^{N}\pi_{ij}\exp(\varphi_j)\right), \quad i = 1,\ldots,N.$$

Next, we will derive the formula for a more general form given by $\mathbb{E}_t^{\mathbb{Q}}\left[h_{t+n}^m \exp(\varphi' s_{t+n-1})|s_t\right]$. Note that for $n \geq 2$, we have

$$h_{t+n}^m = \exp\left(\sum_{k=1}^{n-1} m\rho^{n-1-k}\zeta' s_{t+k} + m\rho^{n-1}\log h_{t+1} + \sum_{k=1}^{n-1} m\rho^{n-1-k} v_{t+k}\right)$$

then

$$\begin{aligned}\mathbb{E}_t\left[h_{t+n}^m \exp(\varphi' s_{t+n-1})|s_t\right] &= \mathbb{E}_t\left[\exp\left(\sum_{k=1}^{n-1} m\rho^{n-1-k}\zeta' s_{t+k} + \varphi' s_{t+n-1} + \sum_{k=1}^{n-1} G(m\rho^{n-1-k})\right)\middle| s_t\right] h_{t+1}^{m\rho^{n-1}} \\ &= \mathbb{E}_t^{\mathbb{Q}}\left[\exp\left(\sum_{k=1}^{n-1}\phi'_{(m,n-1-k,\varphi)} s_{t+k}\right)\middle| s_t\right] h_{t+1}^{m\rho^{n-1}}\end{aligned}$$

where the vector $\phi_{(m,i,\varphi)} \in \mathbb{R}^{N\times 1}$ is defined as

$$\phi_{(m,i,\varphi)} = \begin{cases} G(m\rho^i) + m\rho^i\zeta, & i > 0 \\ G(m) + m\zeta + \varphi, & i = 0. \end{cases}$$

Suppose that, for $n \geq 2$, we have

$$\mathbb{E}_t^{\mathbb{Q}}\left[\exp\left(\sum_{k=1}^{n-1}\phi'_{(m,n-1-k,\varphi)} s_{t+k}\right)\middle| s_t\right] = \exp\left(\theta_n'(m,\varphi)s_t\right),$$

for $n=2$, we have $\theta_2(m,\varphi)=\Delta(G(m)+m\zeta+\varphi)$ from (A.2). For $n=n+1$, we have

$$\begin{aligned}
&\mathbb{E}_t^{\mathbb{Q}}\left[\exp\left(\sum_{k=1}^{n}\phi'_{(m,n-k,\varphi)}s_{t+k}\right)\middle|s_t\right]=\mathbb{E}_t^{\mathbb{Q}}\left[\mathbb{E}_{t+1}^{\mathbb{Q}}\left(\exp(\sum_{k=1}^{n}\phi'_{(m,n-k,\varphi)}s_{t+k})|s_{t+1}\right)\middle|s_t\right]\\
=\;&\mathbb{E}_t^{\mathbb{Q}}\left[\exp\left(\phi'_{(m,n-1,\varphi)}s_{t+1}\right)\mathbb{E}_{t+1}^{\mathbb{Q}}\left(\exp(\sum_{k=2}^{n}\phi'_{(m,n-k,\varphi)}s_{t+k})|s_{t+1}\right)\middle|s_t\right]\\
=\;&\mathbb{E}_t^{\mathbb{Q}}\left[\exp\left(\phi'_{(m,n-1,\varphi)}s_{t+1}\right)\mathbb{E}_{t+1}^{\mathbb{Q}}\left(\exp(\sum_{k^*=1}^{n-1}\phi'_{(m,n-1-k^*,\varphi)}s_{t+1+k^*})|s_{t+1}\right)\middle|s_t\right]\\
=\;&\mathbb{E}_t^{\mathbb{Q}}\left[\exp\left(\phi'_{(m,n-1,\varphi)}s_{t+1}+\theta'_n(m,\varphi)s_{t+1}\right)\middle|s_t\right]=\exp\left(\theta'_{n+1}(m,\varphi)s_t\right),
\end{aligned}$$

with following iterative process

$$\theta_{n+1}(m,\varphi)=\Delta\left(\phi_{(m,n-1,\varphi)}+\theta_n(m,\varphi)\right).$$

Now we obtain

$$\boldsymbol{\Psi}_n(m,\varphi)\equiv\mathbb{E}_t^{\mathbb{Q}}\left(h_{t+n}^m\exp(\varphi' s_{t+n-1})|s_t\right)=h_{t+1}^{m\rho^{n-1}}\exp\left(\theta'_n(m,\varphi)s_t\right).$$

Finally, the formula of $\mathbb{E}_t^{\mathbb{Q}}(h_{t+n}|s_t)$ can be obtained by setting $m=1,\varphi=\mathbf{0}$, such that

$$\mathbb{E}_t^{\mathbb{Q}}(h_{t+n}|s_t)=\exp\left(\rho^{n-1}\log h_{t+1}+\theta'_n s_t\right)=\exp\left(\kappa_n+\rho^{n-1}\log h_{t+1}+\tilde{\theta}'_n s_t\right),$$

with $\kappa_n=\sum_{i=0}^{n-2}G(\rho^i)$, $\tilde{\theta}_1=\mathbf{0}$ and $\tilde{\theta}_{n+1}=\Delta\left(\rho^{n-1}\zeta+\tilde{\theta}_n\right)$. □

B Terms for Analytical Approximation

To simplify the expression, we use the notation $\mathbb{E}_t(\cdot)=\mathbb{E}_t^{\mathbb{Q}}(\cdot|s_t)$ below. Without loss of generality, we set $t=0$, such that T is the number of days to maturity. Now, the conditional moment of cumulative returns $R_T\equiv\log(S_T/S_0)$ is expressed as

$$\mathbb{E}_0\left(R_T^j\right)=\mathbb{E}_0\left[\sum_{i=1}^{T}\left(r-\frac{1}{2}h_{t+i}+\sqrt{h_{t+i}}z_{t+i}\right)^j\right].$$

Expanding the formula, we get

$$\begin{aligned}
\mathbb{E}_0(R_T) &= Tr - \frac{1}{2}\sum_{i=1}^{T}\mathbb{E}_0[h_i], \\
\mathbb{E}_0\left(R_T^2\right) &= T^2r^2 - Tr\sum_{i=1}^{T}\mathbb{E}_0[h_i] + \frac{1}{4}S_{D_1} + S_{D_2} - S_{D_3}, \\
\mathbb{E}_0\left(R_T^3\right) &= T^3r^3 - \frac{3}{2}T^2r^2\sum_{i=1}^{T}\mathbb{E}_0[h_i] + 3Tr\left(\frac{1}{4}S_{D_1} + S_{D_2} - S_{D_3}\right) \\
&\quad + \left(-\frac{1}{8}S_{T_1} + S_{T_2} + \frac{3}{4}S_{T_3} - \frac{3}{2}S_{T_4}\right), \\
\mathbb{E}_0\left(R_T^4\right) &= T^4r^4 - 2T^3r^3\sum_{i=1}^{T}\mathbb{E}_0[h_i] + 6T^2r^2\left(\frac{1}{4}S_{D_1} + S_{D_2} - S_{D_3}\right) \\
&\quad + Tr\left(-\frac{1}{2}S_{T_1} + 4S_{T_2} + 3S_{T_3} - 6S_{T_4}\right) + \left(\frac{1}{16}S_{Q_1} + S_{Q_2} - \frac{1}{2}S_{Q_3} + \frac{3}{2}S_{Q_4} - 2S_{Q_5}\right)
\end{aligned}$$

The formula of S_{D_i}, S_{T_i} and S_{Q_i} are summations of some expectations related to future volatility and shocks that were derived in Duan et al. (1999, p. 104). For instance, the formula of S_{T_2} is given by

$$S_{T_2} = \mathbb{E}_0\left[\sum_{i=1}^{T}\sum_{j=1}^{T}\sum_{k=i}^{T}\sqrt{h_i}z_i\sqrt{h_j}z_j\sqrt{h_k}z_k\right] = 3\sum_{i=1}^{T}\sum_{j=1}^{T-i}\mathbb{E}_0\left[\sqrt{h_i}z_ih_{i+j}\right].$$

The expression requires 19 types of terms as input, which must be derived for the present model. For instance, one type of these terms take the form, $\mathbb{E}_0\left[\sqrt{h_i}z_ih_{i+j}\right]$, and it is needed for the computation of S_{T_2} above. Each of the 19 terms are derived below, and numbered with (B.1)-(B.19).

Expectations without z

We will first derive the formula for following function

$$\begin{aligned}
\mathbb{E}_0\left(h_i^k h_{i+j}^m\right) &= \mathbb{E}_0\left[h_i^k\mathbb{E}_{i-1}(h_{i+j}^m)\right] \\
&= \mathbb{E}_0\left[h_i^k h_i^{m\rho^j} e^{\theta'_{j+1}(m,0)s_{i-1}}\right] \\
&= h_1^{(k+m\rho^j)\rho^{i-1}} e^{\theta_i'(k+m\rho^j,\theta_{j+1}(m,0))s_0} \\
&= \boldsymbol{\Psi}_i\left(k+m\rho^j,\theta_{j+1}(m,0)\right).
\end{aligned}$$

Following Duan et al. (1999), the terms needed for analytical approximation include:

$$\mathbb{E}_0\left(h_i^m\right) = \boldsymbol{\Psi}_i\left(m,0\right), \tag{B.1}$$

$$\mathbb{E}_0\left(h_i h_{i+j}\right) = \boldsymbol{\Psi}_i\left(1+\rho^j, \theta_{j+1}(1,0)\right), \tag{B.2}$$

$$\mathbb{E}_0\left(h_i^2 h_{i+j}\right) = \boldsymbol{\Psi}_i\left(2+\rho^j, \theta_{j+1}(1,0)\right), \tag{B.3}$$

$$\mathbb{E}_0\left(h_i h_{i+j}^2\right) = \boldsymbol{\Psi}_i\left(1+2\rho^j, \theta_{j+1}(2,0)\right), \tag{B.4}$$

and

$$\begin{aligned}
\mathbb{E}_0\left(h_i h_{i+j} h_{i+j+k}\right) &= \mathbb{E}_0\left[h_i \mathbb{E}_{i-1}\left(h_{i+j} h_{i+j+k}\right)\right] \\
&= \mathbb{E}_0\left[h_i h_i^{(1+\rho^k)\rho^j} e^{\theta'_{j+1}(1+\rho^k, \theta_{k+1}(1,0)) s_{i-1}}\right] \\
&= \boldsymbol{\Psi}_i\left(1+\rho^j+\rho^{k+j}, \theta_{j+1}(1+\rho^k, \theta_{k+1}(1,0))\right).
\end{aligned} \tag{B.5}$$

Expectations with z

For terms were z is involved, we define the function

$$\begin{aligned}
\boldsymbol{\Gamma}_i(j,r,m,\varphi) &\equiv \mathbb{E}_0\left(h_i^{\frac{r}{2}} z_i^r h_{i+j}^m e^{\varphi' s_{i+j-1}}\right) \\
&= \mathbb{E}_0\left(h_i^{\frac{r}{2}} z_i^r \mathbb{E}_i\left(h_{i+j}^m e^{\varphi' s_{i+j-1}}\right)\right) \\
&= \mathbb{E}_0\left(h_i^{\frac{r}{2}} z_i^r h_{i+1}^{m\rho^{j-1}} e^{\theta'_j(m,\varphi) s_i}\right) \\
&= \mathbb{E}_0\left(h_i^{\frac{r}{2}} z_i^r e^{\left(m\rho^{j-1}\zeta + \theta_j(m,\varphi)\right)' s_i + m\rho^{j-1}\rho \log h_i + m\rho^{j-1} v_i}\right) \\
&= \mathbb{E}_0\left[h_i^{\frac{r}{2}+m\rho^j} e^{\left(m\rho^{j-1}\zeta+\theta_j(m,\varphi)\right)' s_i}\right] \mathbb{E}_0\left(z_i^r e^{m\rho^{j-1} v_i}\right) \\
&= \mathbb{E}_0\left[h_i^{\frac{r}{2}+m\rho^j} e^{\Delta'\left(m\rho^{j-1}\zeta+\theta_j(m,\varphi)\right) s_{i-1}}\right] \mathbb{E}_0\left(z_i^r e^{m\rho^{j-1} v_i}\right) \\
&= h_1^{a_i(j,r,m)} e^{b'_i(j,r,m,\varphi) s_0} c_i(j,r,m),
\end{aligned}$$

where

$$\begin{aligned}
a_i(j,r,m) &= \left(\tfrac{r}{2}+m\rho^j\right)\rho^{i-1}, \\
b_i(j,r,m,\varphi) &= \theta_i\left(\tfrac{r}{2}+m\rho^j, \Delta\left(m\rho^{j-1}\zeta+\theta_j(m,\varphi)\right)\right), \\
c_i(j,r,m) &= \mathbb{E}_0\left(z_i^r e^{m\rho^{j-1} v_i}\right).
\end{aligned}$$

The expression of $\mathbb{E}_0\left(z_i^r e^{kv_i}\right)$ is provided in Huang et al. (2017, p. 354). So, we have:

$$\begin{aligned}
\mathbb{E}_0\left(\sqrt{h_i}z_i h_{i+j}\right) &= \boldsymbol{\Gamma}_i(j,1,1,0), && \text{(B.6)}\\
\mathbb{E}_0\left(\sqrt{h_i}z_i h_{i+j}^2\right) &= \boldsymbol{\Gamma}_i(j,1,2,0), && \text{(B.7)}\\
\mathbb{E}_0\left(h_i z_i^2 h_{i+j}\right) &= \boldsymbol{\Gamma}_i(j,2,1,0), && \text{(B.8)}\\
\mathbb{E}_0\left(h_i^{3/2} z_i^3 h_{i+j}\right) &= \boldsymbol{\Gamma}_i(j,3,1,0), && \text{(B.9)}
\end{aligned}$$

$$\begin{aligned}
\mathbb{E}_0\left(h_i\sqrt{h_{i+j}}z_{i+j}h_{i+j+k}\right) &= \mathbb{E}_0\left(h_i\mathbb{E}_{i-1}\left(\sqrt{h_{i+j}}z_{i+j}h_{i+j+k}\right)\right)\\
&= \mathbb{E}_0\left(h_i^{1+a_{j+1}(k,1,1)}e^{b'_{j+1}(k,1,1,0)s_{i-1}}c_{j+1}(k,1,1)\right)\\
&= \boldsymbol{\Psi}_i\left(1+a_{j+1}(k,1,1),b_{j+1}(k,1,1,0)\right)c_{j+1}(k,1,1), && \text{(B.10)}
\end{aligned}$$

$$\begin{aligned}
\mathbb{E}_0\left(\sqrt{h_i}z_i h_{i+j}h_{i+j+k}\right) &= \mathbb{E}_0\left(\sqrt{h_i}z_i h_{i+j}\mathbb{E}_{i+j-1}(h_{i+j+k})\right)\\
&= \mathbb{E}_0\left(\sqrt{h_i}z_i h_{i+j}^{1+\rho^k}e^{\theta'_{k+1}(1,0)s_{i+j-1}}\right)\\
&= \boldsymbol{\Gamma}_i\left(j,1,1+\rho^k,\theta_{k+1}(1,0)\right), && \text{(B.11)}
\end{aligned}$$

$$\begin{aligned}
\mathbb{E}_0\left(h_i^{3/2}z_i h_{i+j}\right) &= \mathbb{E}_0\left(h_i\mathbb{E}_{i-1}\left(\sqrt{h_i}z_i h_{i+j}\right)\right)\\
&= \mathbb{E}_0\left(h_i^{1+a_1(j,1,1)}e^{b'_1(j,1,1,0)s_{i-1}}c_1(j,1,1)\right)\\
&= \boldsymbol{\Psi}_i\left(1+a_1(j,1,1),b_1(j,1,1,0)\right)c_1(j,1,1), && \text{(B.12)}
\end{aligned}$$

$$\begin{aligned}
\mathbb{E}_0\left(\sqrt{h_i}z_i\sqrt{h_{i+j}}z_{i+j}h_{i+j+k}\right) &= \mathbb{E}_0\left(\sqrt{h_i}z_i\mathbb{E}_i\left(\sqrt{h_{i+j}}z_{i+j}h_{i+j+k}\right)\right)\\
&= \mathbb{E}_0\left(\sqrt{h_i}z_i h_{i+1}^{a_j(k,1,1)}e^{b'_j(k,1,1,0)s_i}\right)c_j(k,1,1)\\
&= \boldsymbol{\Gamma}_i\left(1,1,a_j(k,1,1),b_j(k,1,1,0)\right)c_j(k,1,1), && \text{(B.13)}
\end{aligned}$$

$$\begin{aligned}
&\mathbb{E}_0\left(\sqrt{h_i}z_i\sqrt{h_{i+j}}z_{i+j}h_{i+j+k}h_{i+j+k+m}\right)\\
=\ &\mathbb{E}_0\left(\sqrt{h_i}z_i\mathbb{E}_i\left(\sqrt{h_{i+j}}z_{i+j}h_{i+j+k}h_{i+j+k+m}\right)\right)\\
=\ &\mathbb{E}_0\left(\sqrt{h_i}z_i h_{i+1}^{a_j(k,1,1+\rho^m)}e^{b'_j(k,1,1+\rho^m,\theta_{m+1}(1,0))s_i}\right)c_j(1,1,1+\rho^m)\\
=\ &\boldsymbol{\Gamma}_i\left(1,1,a_j(k,1,1+\rho^m),b_j(k,1,1+\rho^m,\theta_{m+1}(1,0))\right)c_j(1,1,1+\rho^m), && \text{(B.14)}
\end{aligned}$$

$$\mathbb{E}_0\left(h_i z_i^2 h_{i+j} h_{i+j+k}\right) = \mathbf{\Gamma}_i\left(j,2,1+\rho^k,\theta_{k+1}(1,0)\right), \tag{B.15}$$

$$\mathbb{E}_0\left(h_i h_{i+j} z_{i+j}^2 h_{i+j+k}\right) = \mathbf{\Psi}_i\left(1+a_{j+1}(k,2,1), b_{j+1}(k,2,1,0)\right) c_{j+1}(k,2,1,0), \tag{B.16}$$

$$\mathbb{E}_0\left(\sqrt{h_i} z_i h_{i+j} z_{i+j}^2 h_{i+j+k}\right) = \mathbf{\Gamma}_i(1,1,a_j(k,2,1),b_j(k,2,1,0))\, c_j(k,2,1), \tag{B.17}$$

$$\begin{aligned}
& \mathbb{E}_0\left(\sqrt{h_i} z_i \sqrt{h_{i+j}} z_{i+j} \sqrt{h_{i+j+k}} z_{i+j+k} h_{i+j+k+m}\right) \\
= \; & \mathbb{E}_0\left(\sqrt{h_i} z_i \mathbb{E}_i\left(\sqrt{h_{i+j}} z_{i+j} \sqrt{h_{i+j+k}} z_{i+j+k} h_{i+j+k+m}\right)\right) \\
= \; & \mathbb{E}_0\left(\sqrt{h_i} z_i h_{i+1}^{a_j(1,1,a_k(m,1,1))} e^{b'_j(1,1,a_k(m,1,1),b_k(m,1,1,0))s_i}\right) \\
& \times c_j(1,1,a_k(m,1,1)) c_k(m,1,1) \\
= \; & \mathbf{\Gamma}_i(1,1,a_j(1,1,a_k(m,1,1)),b_j(1,1,a_k(m,1,1),b_k(m,1,1,0))) \\
& \times c_j(1,1,a_k(m,1,1)) c_k(m,1,1),
\end{aligned} \tag{B.18}$$

and finally,

$$\mathbb{E}_0\left(h_i z_i^2 \sqrt{h_{i+j}} z_{i+j} h_{i+j+k}\right) = \mathbf{\Gamma}_i(1,2,a_j(k,1,1),b_j(k,1,1,0))\, c_j(k,1,1). \tag{B.19}$$